AN EXPERIMENTAL STUDY OF NONLINEAR OSCILLATIONS IN RAILROAD FRICTION CONTROL SYSTEMS

by

Mohammad Reza Talebi Bidhendi

B.Sc., Amirkabir University of Technology, 2016

A THESIS SUBMITTED IN PARTIAL FULFILLMENT OF

THE REQUIREMENTS FOR THE DEGREE OF

MASTER OF APPLIED SCIENCE

in

THE FACULTY OF GRADUATE AND POSTDOCTORAL STUDIES

(Mechanical Engineering)

THE UNIVERSITY OF BRITISH COLUMBIA

(Vancouver)

September 2018

The following individuals certify that they have read, and recommend to the Faculty of Graduate and Postdoctoral Studies for acceptance, a thesis/dissertation entitled:

AN EXPERIMENTAL STUDY OF NONLINEAR OSCILLATIONS IN RAILROAD FRICTION CONTROL SYSTEMS

submitted by Mohammad Reza Talebi Bidhendi in partial fulfillment of the requirements for

the degree of Master Of Applied Science

in Mechanical Engineering

Examining Committee:

Dr. A. Srikantha Phani

Supervisor

Dr. Jin Xiaoliang

Supervisory Committee Member

Darren Loo, PENG, Engineering lead, LBFoster representative

Supervisory Committee Member

Abstract

Friction control at the wheel-rail interface has been an outstanding challenge in front of the rail road engineers throughout the world. On-board solid stick friction modifier system, simply named stick-applicator assembly, has proved to be one of the simple and efficient ways to tackle the excessive wear and rail corrugation. Interlocking solid sticks are applied to the wheel flange and tread by means of a mechanical applicator mounted on a bracket, which is connected to the bogie. Relative sliding motion in the stick-wheel interface provokes gradual transfer of solid lubricant film to the wheel-rail interface through the wheel's motion. Consequently, friction control at wheel-rail interface could be achieved. Instability and failure of stick-applicator assembly due to stick-wheel interaction destabilize its performance. The present study uses a lab-scale setup to produce consistent instability, which helps examine the behavior of the stick-applicator assembly during instability. The lab-scale setup incorporates a mock-wheel connected to the stick-applicator assembly. Mock-wheel is used to simulate up - down and transverse motion based on the concept of parametric excitation in the presence of internal resonance. Dynamics of each substructure is investigated to gain better understanding of the behavior of the coupled system. Having known the characteristics of each substructure, the dynamics of the coupled system is studied. It is found that period doubling bifurcation occurs consistently in certain ranges of excitation frequencies and voltages. Lateral stiffness is identified as one of the design parameters of the lab-scale setup that governs the vibration level. Clearances in the stick-applicator assembly and looseness between each interlocking sticks are found to be parameters which weaken the lateral stiffness of the coupled system. Some modifications in the design of the main contributing parts to eliminate instability and suppress the vibration of the coupled system in the lab-scale setup are also addressed in this thesis. Furthermore, full-wheel rig experiments are carried out to check the practicality of the design modifications.

Lay Summary

The idea of using lubricants to reduce the wear and friction at the wheel-rail interface in Vancouver mass transit systems dates back to 1980's when the rails were replaced shortly after the establishment of the mass transit systems due to the huge amount of wear and rail corrugation. Engineers came up with a new idea of exploiting on-board solid stick friction modifier systems suspended from the bogie and connected to the wheel through frictional contact. Relative sliding motion in the stick-wheel interface leads to gradual transfer of solid lubricant film to the wheel-rail interface through the wheel's motion and consequently friction control at wheel-rail interface could be achieved. Problems associated with the stability and failure of friction modifier systems due to stick-wheel interaction undermines their performance. The present dissertation scrutinizes the instability mechanisms and investigates the ways to lower vibration in friction modifier systems by introducing design modification of their components through a lab-scale setup.

Preface

The present thesis entitled “An experimental study of nonlinear oscillations in railroad friction control systems” is original and unpublished work conducted by the author, Mohammad Reza Talebi Bidhendi, under supervision of Dr. A. Srikantha Phani. This project was financially supported by LBFoster Company and Natural Science and Engineering Research Council of Canada (NSERC). Portion of Chapter 2 will be submitted to a pertinent journal in the field. Parts of the same work about insert design modifications presented in Chapter 2 can be patented as a joint contribution with LBFoster Company.

Table of Content

List of Tables

List of Figures

Glossary

Abbreviations

FE	Finite Element
FFT	Fast Fourier Transform
FRF	Frequency Response Function
Aa	Axial Acceleration
La	Lateral acceleration
Va	Vertical acceleration
STFT	Short Time Fourier transform
PD	Period doubling
PSD	Power Spectral Density

Symbols

f	Frequency

Acknowledgements

"It is never a question as to whether it can be done - it is only whether one cares to spend the time and effort"

Clarence Walton Musser

I would like to express my deepest gratitude to my supervisor, Dr. Srikantha Phani, for boosting the sense of being a gladiator in research in me. This project would not have been possible without his encouragement.

I would also like to thank faculty members at UBC, particularly Professor Yousef Altintas and Clarence De Silva, who kindly answered my questions and help me achieve broader view in the field of dynamical systems. I am grateful to my lab-mates at DAL for creating a friendly research atmosphere. I would also like to extend my appreciation to our partners in LBFoster, Mr. Ron Hui, Mr. Darren Loo, Mr. David Elvidge for their important discussions and critical reviews.

I want to take this opportunity to thank Andrew Mckay from university of Cambridge for his suggestions and comments about this project.

Last but not the least, my especial thanks should be given to my parents and sister for supporting me throughout my life.

Dedication

To my parents.

Chapter 1: Introduction

1.1 General overview

Rail road engineers always seek the most effective, inexpensive and secured way to overcome the wheel-rail transportation related problems. These include track life increase, improving fuel efficiency by optimizing traction and train weight, wear decrease and excessive noise suppression during wheel-rail interaction. Friction management at the wheel rail interface has been recognized to be crucial. Several methods of friction modification have been developed and designed by the railway industries including liquid and spray based top of rail friction modifiers by which the top of rail is lubricated, and carbon-based solid stick technology by which wheel flange and tread are lubricated. More details about friction modification in railway transportation can be found in [1,2,3]. The idea of using solid lubricants to reduce the wear and friction at the wheel-rail interface in Vancouver mass transit systems dates back to 1980's when rails were replaced shortly after the establishment due to the huge amount of wear and corrugation [4]. On-board solid stick friction modifier systems suspended from the bogie and connected to the wheel through frictional contact are used to tackle the aforementioned issues (Figure 1.1). Moreover, other features of solid lubricants such as environmentally friendly, fire resistance, non-toxic and low wear rates provoked them to be eminently suitable in freight, urban transit and heavy haul locomotives.

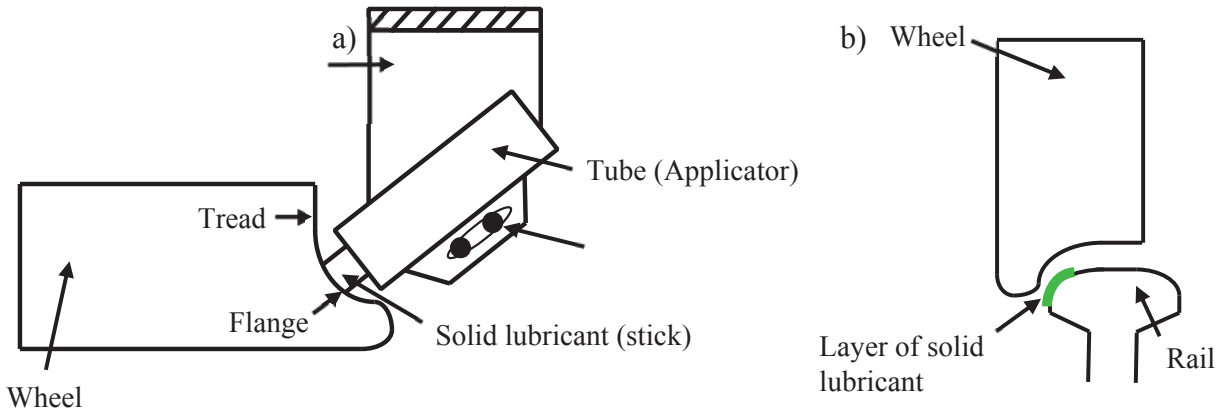

Figure 1.1: A schematic of operation of an on-board solid stick friction modifier system; a) wheel flange lubrication, b) thin transferred solid lubricant film from the wheel to the rail

Although using applicator-stick assembly leads to effective reduction of wear and friction at the wheel-rail interface, stability and failure of the solid stick friction control systems remain a challenging issue that can drop the efficacy of that technology. Stick-applicator assemblies are prone to excessive vibration and noise due to stick-wheel and stick-applicator interaction. Hence eliminating the instability and preventing failure of the stick -applicator assembly by experimental identification of instability mechanisms are the focus of this project.

1.2 Problem statement

As depicted in Figure 1.1, interlocking solid sticks are applied to the wheel flange/ tread by means of a mechanical applicator mounted on a bracket, which is connected to the bogie. As shown in Figure 1.2, applicator is a hollow tube utilizing a folded and removable part named insert with a constant force spring. Sticks are placed inside the applicator and pushed from one side by a constant force spring to be continually in contact with the wheel flange at the other side.

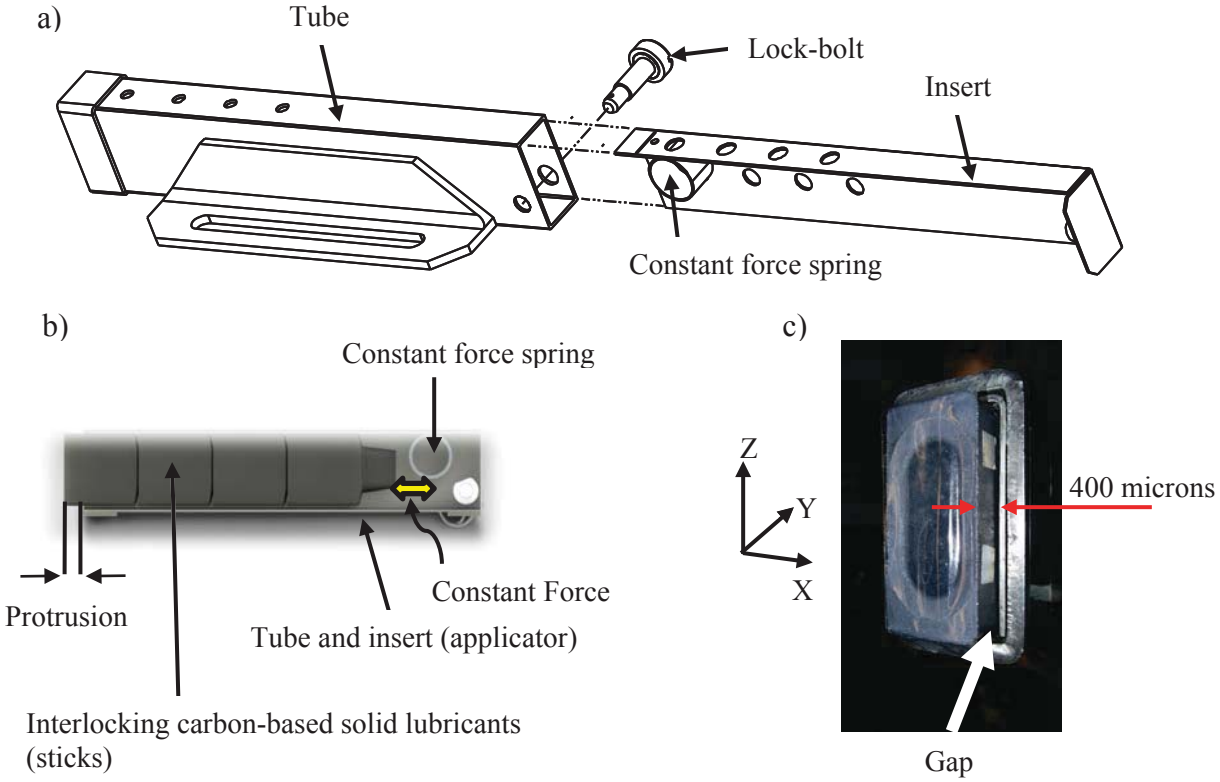

Figure 1.2 : Schematic of the applicator-stick assembly; a) exploded view of the applicator ,b) cross section of a loaded applicator showing interlocking sticks inside the tube, c) front view showing clearance between sticks and insert. Note that free-play exists in X and Z direction.

Excessive amount of stick's vibration, which is the result of the relative motion between the wheel and stick-applicator assembly, is one of the main concerns in dealing with the failure of the mechanical applicators. As shown in Figure 1.2(c), sticks can freely move and hit the internal sides of the applicator because of less constraints in X and Z directions due to the presence of the clearance which exists inevitably in the system due to manufacturing tolerances. Consequently, stick-wheel and stick-applicator interactions may lead to the failure of the applicators through the friction –induced vibration and vibro-impact mechanisms.

In this thesis, practical ways of suppressing the sticks' vibration are explored by performing experiments on a lab-scale setup, which includes a mock-wheel to simulate the relative motion between the wheel and the stick-applicator assembly (Figure 1.4), and available full-scale wheel test-rig at LBFoster Company.

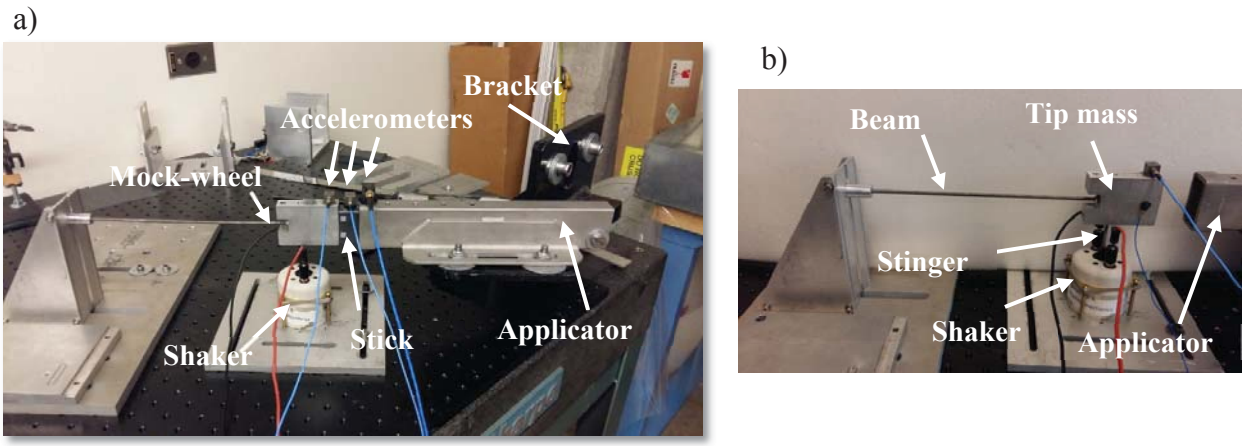

Figure 1.3 : UBC lab- scale experimental setup; a) coupled system, b) uncoupled system

1.3 Literature review

Since the current project deals with three important phenomena including friction-induced vibration due to stick-wheel interaction, vibro-impact oscillation because of stick-applicator interaction and nonlinear mechanisms route to instability due to the mock-wheel's dynamics, a brief pertinent literature review is given in the following subsections.

1.3.1 Friction – induced vibration and instability

Friction-induced vibration and instability is usually known as the root cause of undesired noises and instabilities in many engineering applications such as disc-brake interaction in automotive industry, machining processes, wheel-rail interactions, ceramic-on-ceramic hip arthroplasty, etc. Numerous studies have been conducted and various models have been proposed to describe the behavior of the systems oscillating due to friction. Friction modeling is a key task for the mathematical models to successfully predict the system's behaviors with frictional contact [5]. The underlying mechanisms of friction generated instability and chaos have been comprehensively reviewed in [6,7,8,9]. Some of the mechanisms are briefly presented here.

1.3.1.1 Negative slope of friction coefficient

When friction coefficient is a decreasing function of relative velocity of two sliding systems in contact, friction can be interpreted as a negative damper feeding energy to the system instead of dissipating it. This characteristic was recognized to be an essential destabilizing mechanism for a long time [7]. However, Jarvis and Mills [10] showed that decreasing of friction coefficient with sliding speed could not alone amount for the squeal, based on their setup consisting of a cantilevered beam on a unidirectional rotating disc. Geometry of the coupling of the motions was identified as the main cause of instability in their setup. Moreover, Chen et al [11] looked at the instabilities arising from the frictional interaction of a reciprocally driven pin-on-plate apparatus and observed squeal occurrence in both regions of negative and positive friction-velocity gradients but no clear explanation was given.

1.3.1.2 Stick-slip

Stick-slip motion, a non-smooth behavior, usually occurs at a low sliding speed between two surfaces due to the difference between the static friction coefficient and the kinetic friction coefficient or transition between elastically deformed asperities during sticking phase followed by plastically deformed asperities during sliding phase. Stick-slip vibration occurs in many systems such as drill strings in oil and gas well drilling [12], brake system, and bowed music instruments. In some cases, stick-slip vibration alone cannot be the source of brake squeal noise, but it can lead to the coupling of various modes in the system by releasing an impact-wise energy during slipping phase and enhance the squeal propensity [13, 14]. Hence, finding its causes and avoiding its formation by changing system parameters including interface frictional properties are pursued in industrial applications.

1.3.1.3 Mode coupling

Flutter is a common example of mode coupling when at least two closely spaced modes of a system, get coupled and merge into one due to certain conditions such as having an asymmetric stiffness and/or damping coefficient matrices arising from follower loads or frictional contact conditions. Akay et al [15] demonstrated mode coupling as one of the most important mechanisms in the disc brake squeal and the effect of damping in the squeal noise through a simplified designed test rig. F.Chen [16], by using the concept of aligned frequencies, demonstrated that the squeal frequency is close to the aligned frequency. He addressed that if one in-plane mode of the rotor falls into the less than one-third frequency distance between the two adjacent out-of-plane rotor's modes, in-plane and out-of-plane modes are said to be aligned and there is a high possibility of squeal to arise if a proper friction, pressure and temperature exist to couple those modes. Hoffman [17] studied a minimal two degree of freedom model exhibiting mode coupling instability. Flutter route to instability has also been observed by several researchers in follower loading structures, both experimentally and theoretically [18,19].

The above mechanisms are the accepted and identified sources of the instability in engineering systems. However, nonlinear mechanisms route to instability including modal interactions (internal resonances), parametric oscillations, subharmonic or super harmonic

resonances are also known to be involved in dynamical systems and some of them are discussed briefly in section 1.3.3.

There is a strong analogy between the wheel-stick-applicator assembly and disc-brake system, widely discussed in the literature. Train wheel, applicator and sticks can be treated as disc, caliper and pads respectively. Although controlling friction at the wheel-rail interface is done by the stick-applicator assembly, the physics behind the chatter/squeal occurrence in wheel-stick-applicator assembly remains unresolved. Inspired by the linear stability theory in frequency domain used by Duffor and Woodhouse [20] in studying the disc brake squeal and Altintas [21] in constructing the stability lobes for milling process, the first rudimentary work in the context was done by Sharma et al [22]. He studied the stability of an applicator mounted on three different brackets in contact with the wheel in a virtual environment. Further, he did modal experiments to measure the required transfer functions for the linear stability theory. No chatter/squeal was observed during his field experiments and he mentioned the wheel-stick interaction as a forced vibration process. Robustness of his model is under question since the stick's influence, clearances as one of the main sources of the nonlinearities and vibro-impact phenomena were neglected in his model. The effect of sticks and clearances are studied in the present work by the lab-scale setup (Figure 1.4).

1.3.2 Vibro- impact phenomena

Woodpecker toy [23], ground moling [24], impact dampers [25] and various loosely connected structures have been studied as typical examples of vibro-impact phenomena. Clearances in loosely connected systems similar to the stick-applicator apparatus can prompt the vibro-impact effects which results in noise level increase during operation and fatigue intensification of components. Impact dampers used in machining process to passively suppress the unwanted vibration (chatter) [26, 27], however, are one of the desired application of vibro-impact phenomena. A single mass can act as an impact damper in systems with clearances (Figure 1.5) by absorbing part of the main oscillating system's energy during impact.

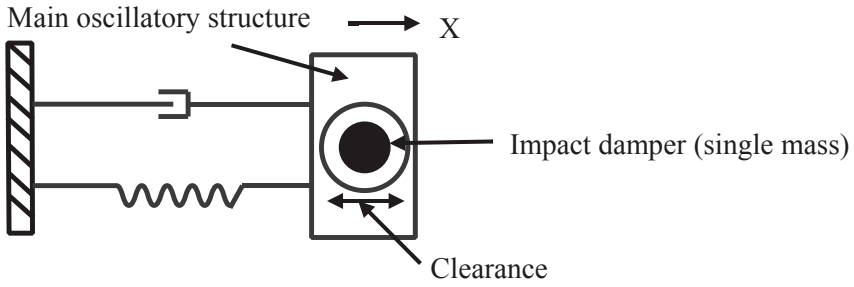

Figure 1.4 : A vibration model of drill with impact damper; note that in some cases impact damper can be equipped outside of the main oscillatory system as well [27]

In general, vibro-impact phenomenon is a non-smooth process and can be a nonlinear mechanism leading to instability. Many complex behaviors such as drift in response, subharmonic response and chaotic motion might potentially be observed in certain conditions and due to system's parameters in an impact oscillator [28, 29].

Stick-applicator assembly can be treated as an impact oscillator due to the existence of the clearance between the stick and the applicator. To prevent the failure of the applicators caused by the stick motion, inserts may be designed to act as an impact damper to absorb stick's energy. Different types of inserts are studied in this work.

1.3.3 Non-linear mechanisms route to instability

Nonlinearity is an ubiquitous characteristic in most practical engineering systems. Large deformation of structural elements such as beams, shells and plates, impact and backlash and elasto-plastic behavior of materials exemplify the geometric, non-smooth and material nonlinearities in the systems respectively. Identification of nonlinearities and their influence on system operation is of great importance in achieving proper and simple models to predict the system's behaviors adequately. Furthermore, there are involved phenomena exclusive to nonlinear systems and using linear models for that systems lead to spurious results. Modal interaction (internal resonance), saturation, amplitude dependent frequency of oscillation, jump (hysteresis) ,subharmonic or super harmonic resonances due to certain circumstances can arise only in nonlinear systems. A brief review of one of the known features of nonlinear structures associated

with the current project, in particular the mock-wheel used in the lab scale setup, are provided here. More details can be found in [30].

1.3.4 Internal resonances

Modal interactions occur in nonlinear multiple degree of freedom systems as a result of the presence of the internal coupling and energy exchange between the modes due to nonlinearities. Autoparametric or internal resonances, which is one type of modal interaction in nonlinear systems, is said to exist when two or more of a system's linear natural frequencies are commensurate or nearly commensurate, i.e. $\omega_2 \simeq 2\omega_1, \omega_3 \simeq 3\omega_1 \pm \omega_2$. Internal resonances depend on the order of the nonlinearities. For instance, when a structure has a quadratic damping or an asymmetrical geometry caused quadratic nonlinearity, internal resonances may be anticipated if $\omega_m \simeq 2\omega_n \, or \, \omega_m \simeq \omega_n \pm \omega_k$, while for cubic nonlinearities such as cubic stiffness, internal resonances arise when $\omega_m \simeq 3\omega_n \, or \, \omega_m \simeq 2\omega_n \pm \omega_k$. Internal resonances, which can be a nonlinear mechanism route to instability, when combined with external resonance can cause hazardous large responses in modes and enhance fatigue-related problems. However, they have been purposefully exploited in applications including vibration absorption [31] and energy harvesting [32, 33]. A two-DOF model (Figure 1.6) was widely used as a good approximation to explain the observed behaviors including saddle-node bifurcation (jump phenomenon), Hopf bifurcation, Period doubling (PD) bifurcation, saturation and chaotic motion during experiments on the autoparametric systems [31,34,35]. Fourier spectra, time-frequency analysis, time histories, autocorrelation for detection of chaotic motion, Poincare sections and maps are useful tools in characterizing the responses of nonlinear systems [36, 37].

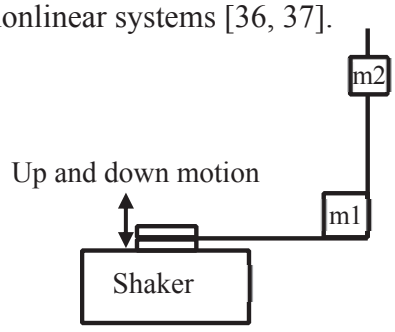

Figure 1.5 : Adjusted two-degree of freedom model for a 2:1 autoparametric resonance investigated by Nayfeh [35]

The mock-wheel designed in the current work draws on the approach of a 2:1 autoparametric resonance with new boundary conditions. The mock-wheel shows some fascinating responses such as jump phenomenon (Hysteresis) and period doubling bifurcation in certain frequency ranges by increasing the excitation level which are discussed in Chapter 2 of this dissertation.

1.4 Objectives and outline

As mentioned earlier, chatter/squeal was not observed during the stick-wheel interaction by Sharma [22]. Moreover, it was reported to be an inconsistent phenomenon in the field experiments by the industry. Therefore, the lab scale setup (Figure 1.4), which uses mock-wheel as a parametric system in the presence of internal resonance to simulate up-down and transverse motion, is opted for producing consistent instability. The objective of this work is to understand how stick-applicator assembly performs at instability. Next, how to eliminate the instability of the applicator-mock-wheel assembly and suppress the vibration by identifying the contributing design factors and hence modifying the main contributing parts such as sticks, clearances and inserts are addressed based on the lab scale setup. Furthermore, full scale test rig is also used to check the usefulness of conclusions made according to the lab-scale setup findings.

The current dissertation is organized as follows: in Chapter 2, the components of the lab-scale setup is described along with modal experiments and Finite Element (FE) simulations to extract the linear natural frequencies and investigation of mock-wheel nonlinear behavior. After that, the dynamics of the applicator-mock-wheel assembly is analyzed experimentally to highlight the main contributing parts of stick-applicator assembly. In Chapter 3, the results of experiments conducted on the full-wheel test rig are presented and practicality of conclusions made based on the lab-scale setup findings is assessed. Finally, conclusions are recapitulated in Chapter 4.

Chapter 2: Lab-scale Experiments and Modeling

Chatter/squeal occurrence due to stick-wheel interaction was reported to be an inconsistent (not repeatable) phenomenon in the field experiments. Furthermore, most of vibration arising from stick-wheel interaction is said to be forced vibration [22]. Therefore, it could be reasonable to conclude that rotational motion of the wheel ,as a source of energy in stick-wheel interaction, may not be the main reason of producing instability in the field experiments. Wheel's suspension motion, as another source of energy in the stick-wheel interaction, could be responsible for the instability in the field experiments. Inspired by the train wheel-suspension motion, mock-wheel was designed. As shown in Figure 1.4, the lab-scale setup using the mock-wheel to provide relative motion is exploited to produce consistent instability. The setup also helps to understand the practical ways to suppress vibration in applicator-mock-wheel assembly by modifying the parts of stick-applicator assembly. Knowing the dynamics of each subsystem used in the applicator-mock-wheel assembly is the first step toward the analysis of the coupled system. Therefore, this chapter begins with the description of each substructure used in the coupled system along with the experimental vibration testing to characterize their linear and nonlinear dynamics . Finite element (FE) models are also used to determine the linear mode shapes of each substructure and verify the experimentally measured natural frequencies. In section 2.2, experimental procedures and analysis conducted on the coupled system are described. This is followed by identifying and modifying the main contributing parts including sticks, clearances and inserts to eliminate instability and decreasing the vibration level in the whole system.

2.1 Substructures in the coupled system

2.1.1 Mock-wheel

Inspired by the train wheel-suspension motion, mock-wheel was designed to provide a relative motion in the coupled system. Mock-wheel includes a cantilevered beam with an aluminum tip mass connected to an electromagnetic shaker (LDS V101) by a stinger (Figure 2.1).

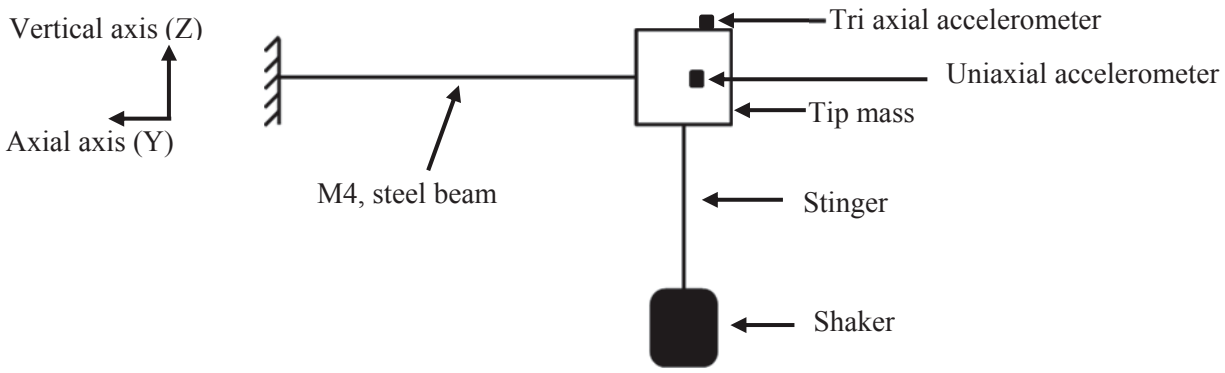

Figure 2.1 : Schematic of the mock-wheel and its components

Shaker provides up and down sinusoidal motion. The cantilevered beam and the shaker's vertical stiffness act as suspension stiffness and tip mass is representative of the wheel. Since shaker is deemed part of the mock-wheel, shaker-structure interaction analysis is neglected in this section.

2.1.1.1 Linear natural frequencies and mode shapes

Natural frequencies of the mock-wheel are extracted by applying both low-level swept-sine excitation signal through the shaker and impulse tests. To get accurate natural frequencies, sweep rate should be monitored to have less influence on the results [38]. The in-house logger software is used to identify the natural frequencies from the experimentally measured Frequency Response Functions (FRF) and response of the mock-wheel illustrated in Figure 2.2. A tri-axial accelerometer whose sensitivities in three directions are very close to each other (98 mv/g) is mounted on the tip mass to measure the acceleration in three orthogonal directions.

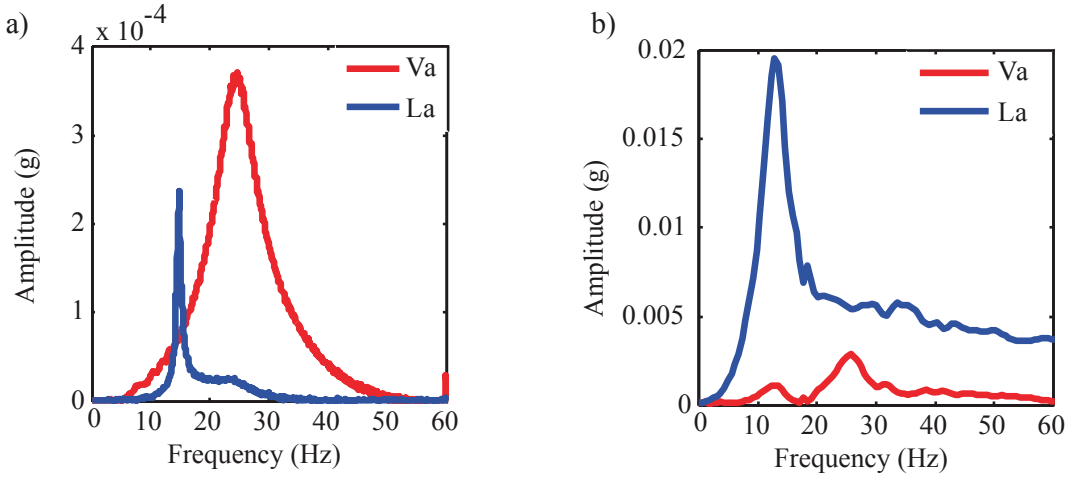

Figure 2.2 : Frequency spectrum of the mock-wheel with respect to the different excitation inputs; a) response of vertical low-level sine sweep excitation signal, b) response due to impact applied on the lateral side of the tip mass. Note that response amplitudes are different since input excitations and the point they are applied are different. Va and La are vertical and lateral acceleration respectively.

Coherence function, as a measure to show how well the output (response) is related to the input (impulse) linearly, is also calculated by repeating the impulse tests to indicate the accuracy of the measurements. A good coherence at resonance peaks is achieved (Appendix I).

A 3D FE model created in ABAQUS and relevant mode shapes based on considering the shaker as a unidirectional spring with the stiffness of 3150 N/ m (see Appendix for further details) are illustrated in Figure 2.3. The connecting point between the spring (shaker) and the stinger is constrained to have only vertical motion and the longer beam is clamped at one end. Table 2.1 shows the parts characteristics.

Table 2.1: Modeling parameter for Mock-wheel's FEA

Part	Material property (GPa, kg/ m^3)	Dimensions
Long beam	Young's Modulus =200,Poisson's ratio :0.3, Density : 7800	M4, 25.4 cm
Tip mass	Young's Modulus =71,Poisson's ratio :0.33, Density : 2700	6.98*4.97*1.98 cm^3
Stinger	Young's Modulus = 200,Poisson's ratio :0.3 Density : 7800	M4, 3.98 cm
Shaker	Stiffness : 3150 N/m	----------

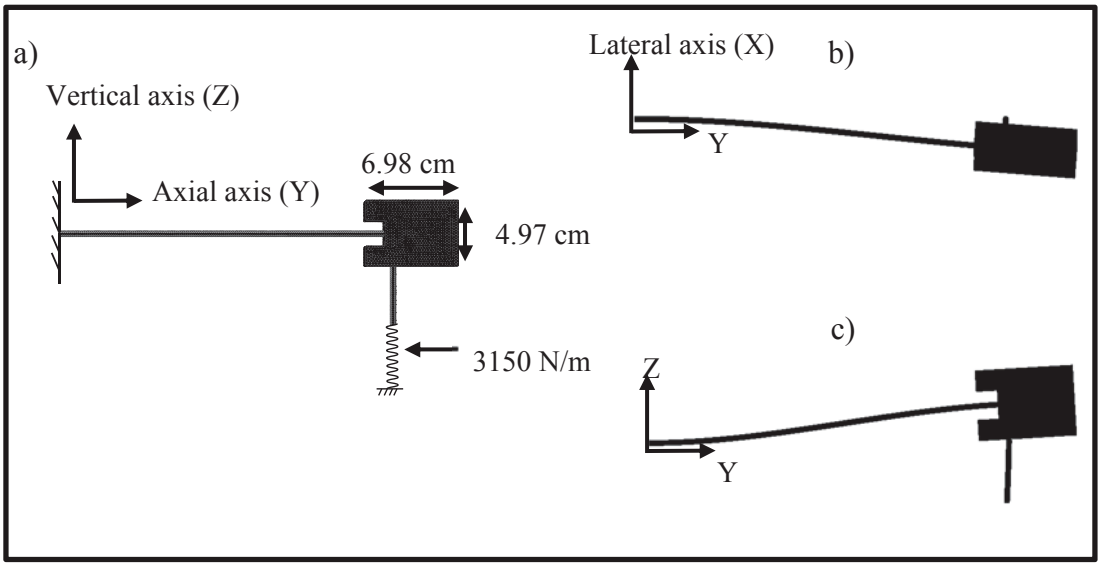

Figure 2.3: Mock-wheel; a) FE model in ABAQUS, b) first lateral bending mode (17.41 Hz), c) first vertical bending mode (24.52 Hz)

Comparisons are made between the FEA frequencies and those extracted experimentally using swept-sine excitation signal with low excitation amplitude and impact hammer testing in Table 2.2. It is worth mentioning that the discrepancy observed in FEA results and experiments can be associated with the modeling approach where shaker is simply replaced by a unidirectional spring. Moreover, the difference between results of the sine-sweep experiments and impact hammer testing can be referred to the fact that the lateral impact directly excites lateral modes whereas vertical excitation in sine-sweep experiments may excites lateral modes (could be treated as cross FRFs).

Table 2.2 : Natural frequencies of the mock-wheel in Hz

Mode	FEA	Swept-sine excitation	Impulse test
1	17.41	14.78	12.36
2	24.52	24.39	25.14

2.1.1.2 Nonlinear behavior of the mock-wheel

Presence of nonlinearities is an inherent property of many real engineering structures and inapplicability of linear techniques to explain complex phenomena including jumps, saturation, limit cycles, internal resonances and chaos behooves the researchers to focus on nonlinear system identification. Nonlinear system identification process, in general, is comprised of three main stages of detection, characterization and parameter estimation (quantification) of nonlinearities [39]. There are standard experimental ways such as FRF variations in frequency domain or lack of proportionality in time responses due to different constant excitation levels and existence of harmonics in response of a system subject to a sinusoid to detect if a nonlinearity presents or not [38,39]. Advanced techniques including construction of backbone curves which demonstrate the amplitude- natural frequency variations and time-frequency analysis using short-time Fourier transform (STFT) and in particular wavelet transform to capture nonstationary effects are also used to characterize and quantify the nonlinearities [40-42]. Nonlinear behavior of the mock-wheel is

studied briefly in this section through detection and characterization of nonlinearities, after briefly explaining the interconnection between parametric oscillation and internal resonance phenomenon which are involved in the mock-wheel's dynamics. Quantification of the nonlinearities (i.e. understanding the onset of jump and construction of back-bone curves) in the mock-wheel is postponed for future studies.

A system is said to be parametrically excited when an internal parameter of a system such as stiffness is an explicit function of time. Pendulum with moving support and buckled axially loaded structures are common examples of parametric oscillation. Once a system is parametrically excited at a certain threshold of the amplitude, the ensuing motion is unstable and grows exponentially if a rational relationship exists between the frequency of parametric excitation and natural frequency of the system. Principal parametric resonance is said to occur above a certain excitation amplitude if the dominant frequency of the response becomes one-half that of the excitation frequency.

Parametric oscillation can occur both in linear and nonlinear systems. Mathieu- Hill equation (equation 2.1) is a universal example of parametric oscillation in linear systems. Axially loaded buckled beams demonstrate parametric oscillation in nonlinear systems. Many researchers such as Floquet have explored stability analysis and construction of stability charts for linear and nonlinear systems with periodic parameters within the last decades. More details are elucidated in [30, 31].

$$\ddot{u} + (a + b\cos(\omega t))u = 0 \qquad (2.1)$$

As pointed out in literature review in Chapter 1, autoparametric or internal resonances, which is one type of modal interaction in nonlinear systems, is said to exist when two or more of a system's linear natural frequencies are commensurate or nearly commensurate. In case of having internal resonance (for instance $\omega_2 = 2\,\omega_1$ or $\omega_2 = \omega_1$) and in the presence of appropriate nonlinear coupling terms including quadratic nonlinearities in a system, second mode of the system can parametrically excite the first mode or vice-versa leading to instability. It is shown later in this section that when mock-wheel is excited vertically in the vicinity of the first vertical mode, which is roughly twice the first lateral mode, there is a threshold above which first lateral bending mode gets excited parametrically.

The time responses (acceleration of tip mass) of mock-wheel in vertical direction (Z axis) to swept-sine excitation of various voltages with the same sweep rate are plotted in Figure 2.4. Absence of proportionality in time responses from 400 mv to 800 mv of excitation, shift in the resonance peak to higher frequencies due to increase in the amplitude of excitation voltages (frequency-amplitude dependence behavior), sudden reduction in response around 26 Hz and asymmetric response around the equilibrium axis (i.e. vertical acceleration of 0) at resonance peak prove the presence of nonlinearities in the mock-wheel. Note that linear sine-sweep signal is used to excite the system, hence, time is converted to sweep frequency according to the sweep rate [42].

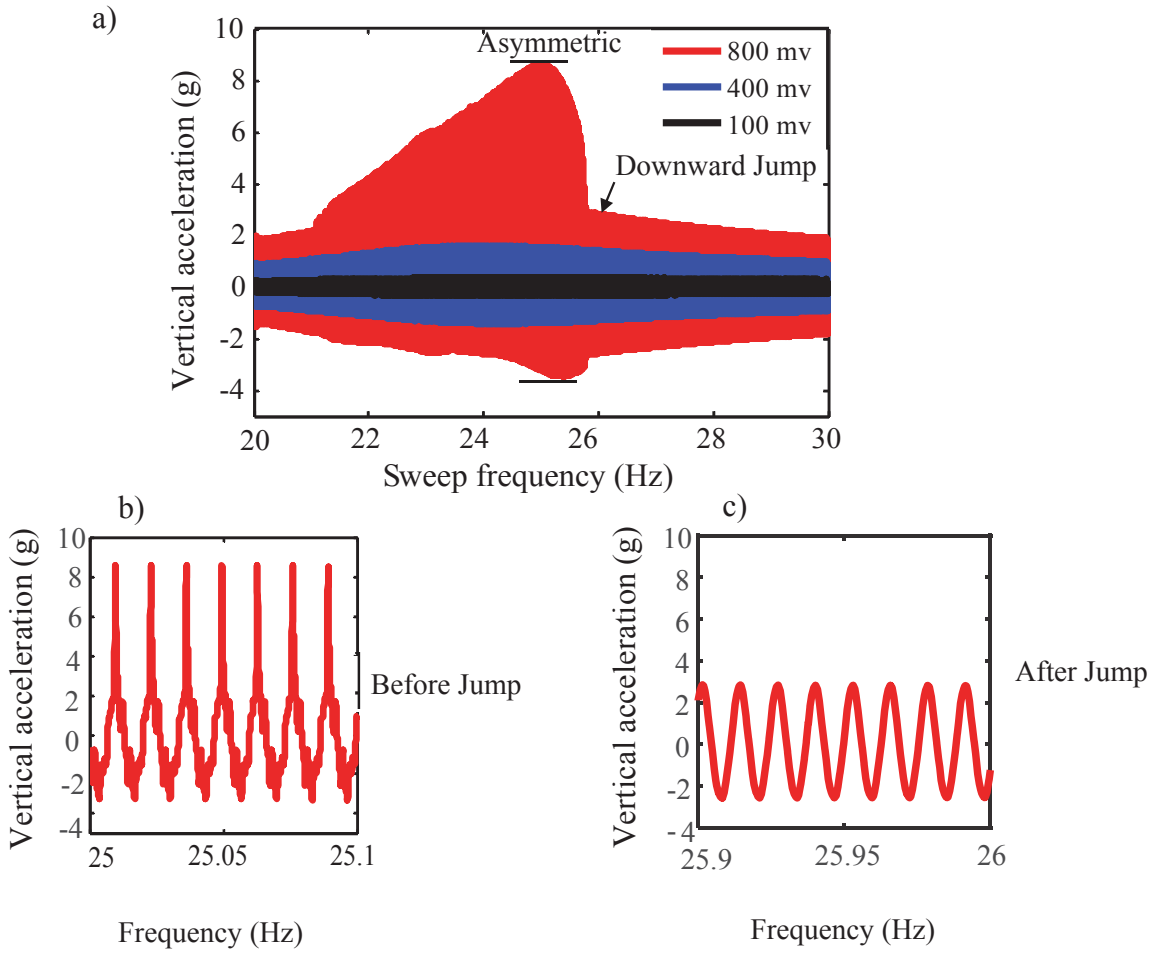

Figure 2.4 : Detection of nonlinearity in mock-wheel's vertical motion by increasing the amplitude of forward sine-sweep excitation (20 Hz to 30 Hz), (b) nonlinear response (acceleration) at 800 mv excitation voltage (before jump), (c) linear response (acceleration) at 800 mv excitation signal (after jump)

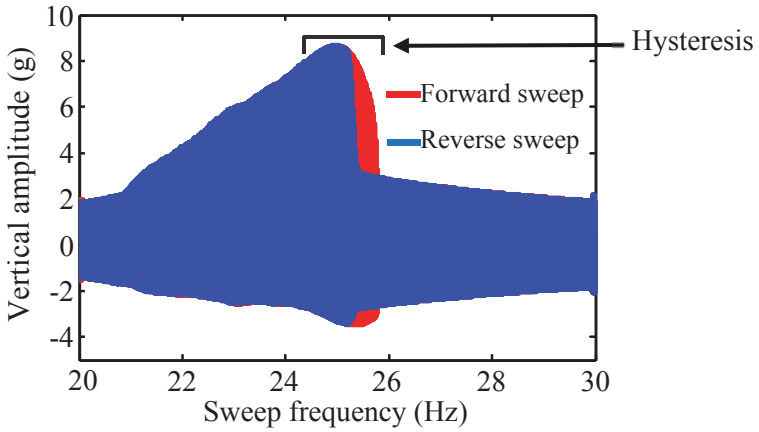

Figure 2.5 : Detection of hysteresis in mock-wheel's vertical motion by comparing the forward and backward sine-sweep excitation (20 Hz to 30 Hz) with 800 mv amplitude

Observation of jump phenomenon in the response and transition from nonlinear response to the linear response by varying the excitation frequency at higher excitation amplitudes are indications of **saddle-node bifurcation**. Figure 2.5 shows hysteresis effect as a further proof of the existence of saddle-node bifurcation, which can be recognized by reversing the order of frequencies in the sweep-test.

Shift of natural frequency to the right by increasing the excitation voltages was also observed but it is not clear in Figure 2.4. It manifests the nonlinearity entails hardening nonlinearity arising possibly from the large deflections in the mock-wheel. However, hardening nonlinearity may not be the only type of nonlinearity in the mock-wheel. It is discussed in this section that even order nonlinearities are also involved in the mock-wheel due to the observation of even order harmonics in the frequency spectrum of the mock-wheel.

Other behavior observed is period-doubling bifurcation, which is known to be one of the routes to chaos, above a certain excitation amplitude threshold. Figure 2.6 illustrates the appearance of subharmonic response at higher excitation amplitudes when the excitation frequency is 24 Hz which is approximately twice the first lateral bending mode of the mock-wheel or in the vicinity of the first vertical mode of the mock-wheel. The responses were measured by the tri-axial accelerometer mounted on the tip mass.

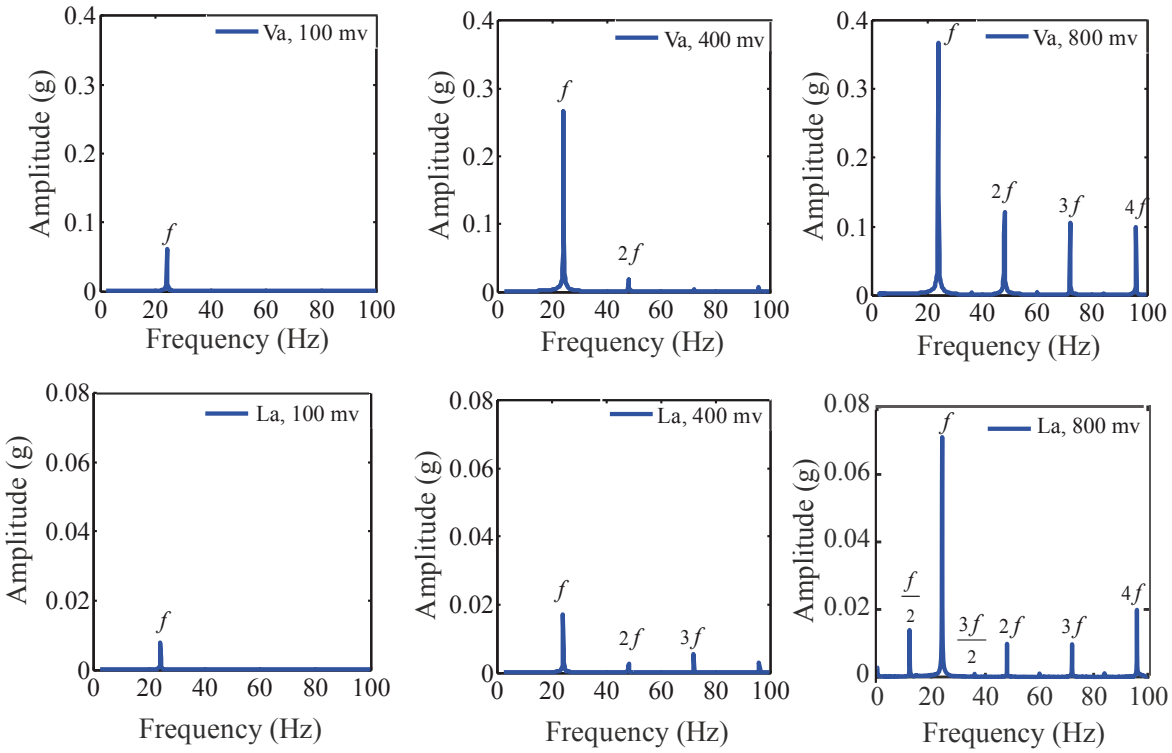

Figure 2.6 : Vertical (first row) and lateral (second row) acceleration of the mock-wheel measured by the tri-axial accelerometer mounted on top of the mock-wheel at different excitation amplitudes at 24 Hz.

It can be hypothesized from above figures that vertical motion causes subharmonic response in the lateral direction at higher excitation voltages. To make sure that parametric resonance occurs in the mock-wheel (i.e. first lateral bending mode becomes unstable), the amplitude sweeps experiment proposed by Zavodney [43] is conducted at 24 Hz. Figure 2.7 presents the variation of Rms values of the acceleration measured by the tri-axial accelerometer on the tip mass as excitation voltage is increased.

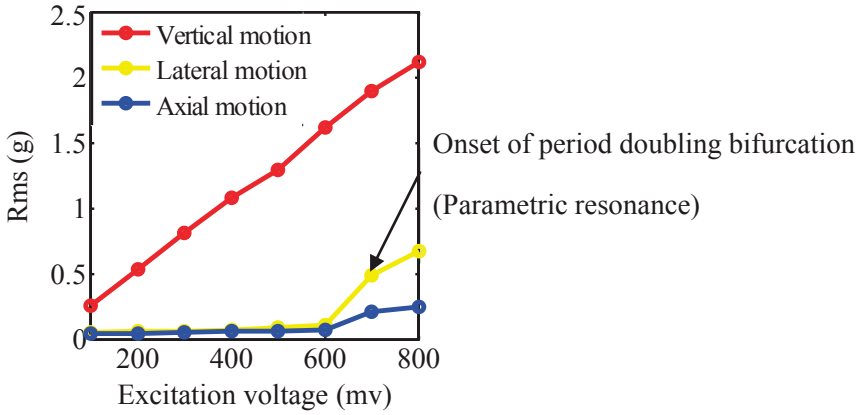

Figure 2.7 : Rms values of mock-wheel acceleration at sdifferent excitation voltages at 24 Hz

Observation of the sudden increase in the response after 600 mv accompanied by period doubling bifurcation indicates parametric resonance in the mock-wheel [43]. Furthermore, lateral displacement and velocity were measured using scanning Vibrometer (PSV 400) to verify that the dominant frequency in the response is half of the excitation frequency (Figure 2.8).

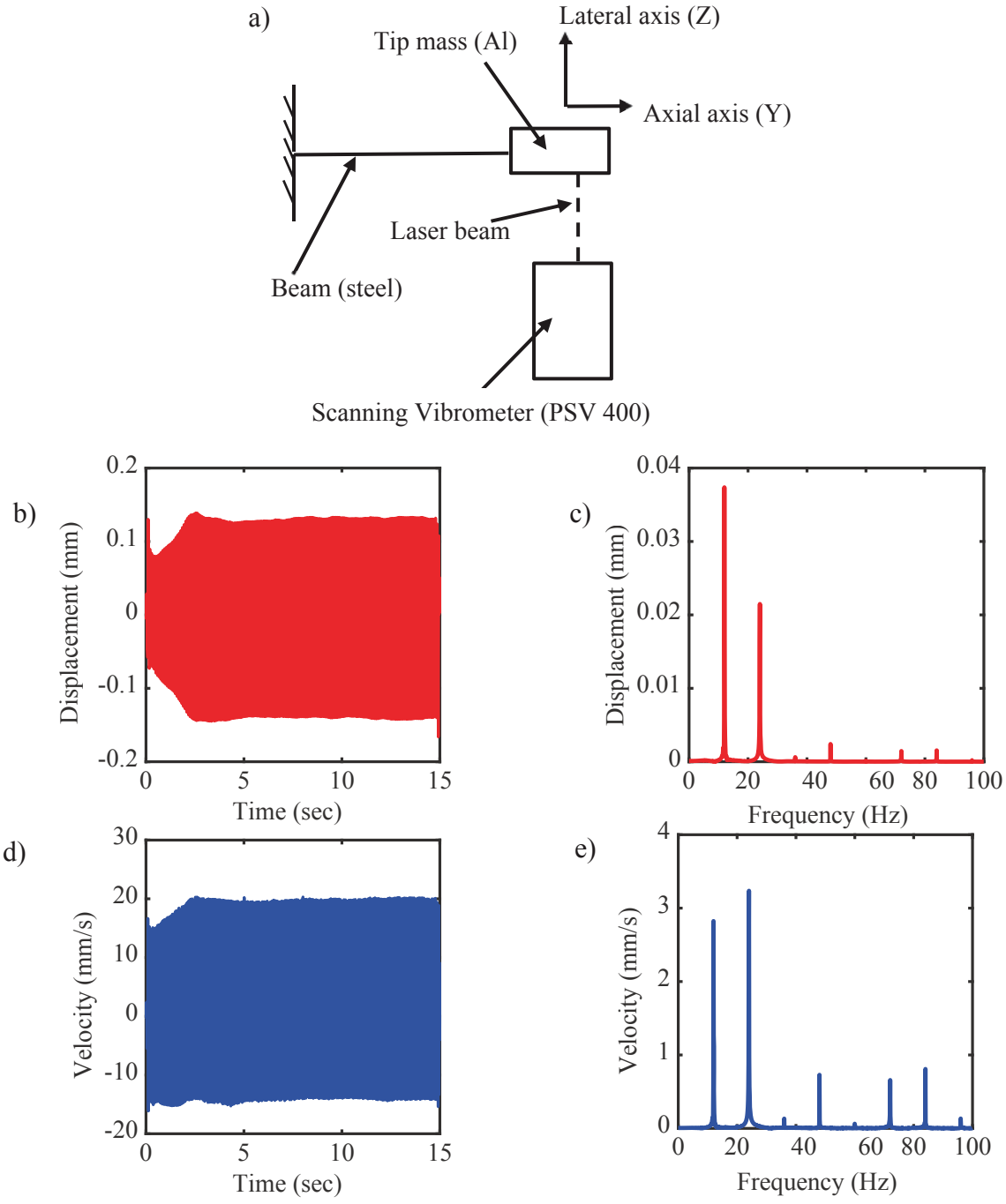

Figure 2.8 : Using laser Vibrometer to capture the lateral displacement and velocity of the mock-wheel. Excitation signal is a sinusoid of frequency 24 Hz and amplitude 800 mv; (a) schematic of the experiment, (b) lateral displacement in time domain, (c) FFT of the lateral displacement, (d) lateral velocity in time domain, (e) FFT of the lateral velocity

From the above figure, it can be observed that when a first vertical mode at 24 Hz is excited, there is a threshold above which vertical mode parametrically excites lateral motion due to 2: 1 modal interaction. Laser Vibrometer was used to show this effect that confirms the presence of quadratic nonlinearity in the system [43]. Note that tri-axial accelerometer showed period doubling (Figure 2.5) but its peak's amplitudes in frequency spectrum are different from the results measured by the laser Vibrometer. That may have to do with the distortions occurring during sensing the lateral motion by the trial-axial accelerometer and position of the tri-axial accelerometer, which was mounted on the top of the tip whereas laser vibrometer measures lateral displacement at the lateral side and middle of the tip mass.

2.1.1.3 Summary of the tests on mock-wheel

Experiments conducted on the mock-wheel to characterize its linear and nonlinear behavior were discussed in detail. Finite element models were used to verify the experimentally measured natural frequencies. It was also shown that mock-wheel includes both hardening nonlinearities such as cubic nonlinearity and even order nonlinearities including quadratic nonlinearity. There was a threshold for the mock-wheel at roughly twice the first lateral bending mode or close to the first vertical mode where parametric resonance occurs. This phenomenon is known as parametric excitation in the presence of 2:1 internal resonance.

2.1.2 Stick- applicator assembly

The detailed structure of stick- applicator assembly was earlier demonstrated in Chapter 1 (Figure 1.2). Applicator is a hollow tube containing a folded and removable part named insert with a constant force spring. Sticks are placed inside the applicator, and from one end they are pushed by the constant force spring to be continually in contact with the wheel flange at the other end. Geometrical properties of different sticks tested in this work are tabulated in Table 2.3 and Figure 2.9 presents different stick designs. Since the sticks are pushed out by the constant force spring, it is impossible to use impact hammer to find the natural frequencies of the loaded applicator. The only way to experimentally gain the approximate system's modes is to apply unidirectional excitation force parallel to the axial axis (longitudinal axis) of the applicator by an electromagnetic shaker. However, it will be shown later both experimentally and by using FEA that stick-insert assembly might explain the modes found by the unidirectional excitation test (axial test) in section 2.1.2.2.

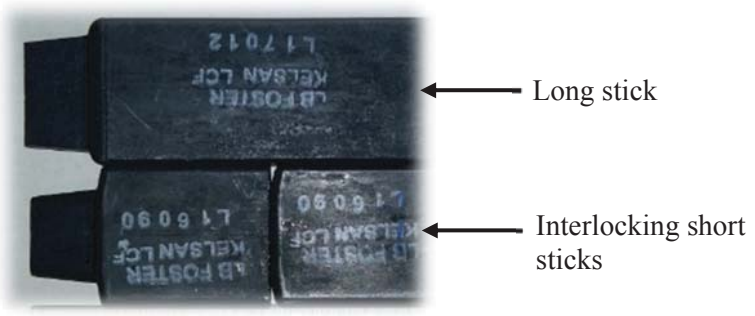

Figure 2.9 : Geometrical properties of the sticks tested in the current work

Table 2.3 : Geometrical properties of different sticks

sticks	Weight	Length
1 Short stick	90 grams	73.45mm
1 Long stick	183 grams	126mm
2 Short sticks	180 grams	125mm
4 Short sticks	362 grams	232mm

2.1.2.1 Axial test

Stick-applicator assembly, intrinsically, is a nonlinear structure due to the presence of clearances between the sticks and the insert/applicator (Figure 1.2 (c)). Some techniques in shaker testing including, using an appropriate stinger and force sensor are exploited to gain accurate and reliable results during modal experiments by applying low level of excitation (50 mv) to prevent the intensification of nonlinearities. The setup illustrated in Figure 2.10 utilizes a tri-axial accelerometer (98 mv/g) on top of the protruded stick to measure the cross and direct FRFs in vertical, lateral and axial direction. Special attention should be given to find the lateral and vertical modes since it is possible to observe apparent and false peaks in the cross transfer functions due to the force drop off during the natural resonance of the structure in the axial direction, cross sensitivity of the accelerometer and slight misalignment between the stinger and the structure. Moreover, to minimize the shaker-structure interaction, proper stinger was designed to have resonances well beyond the structures' resonances but not too stiff to contaminate the results. Force sensor (100 mv/N) was also used to decouple the shaker-stinger assembly from the stick-applicator assembly.

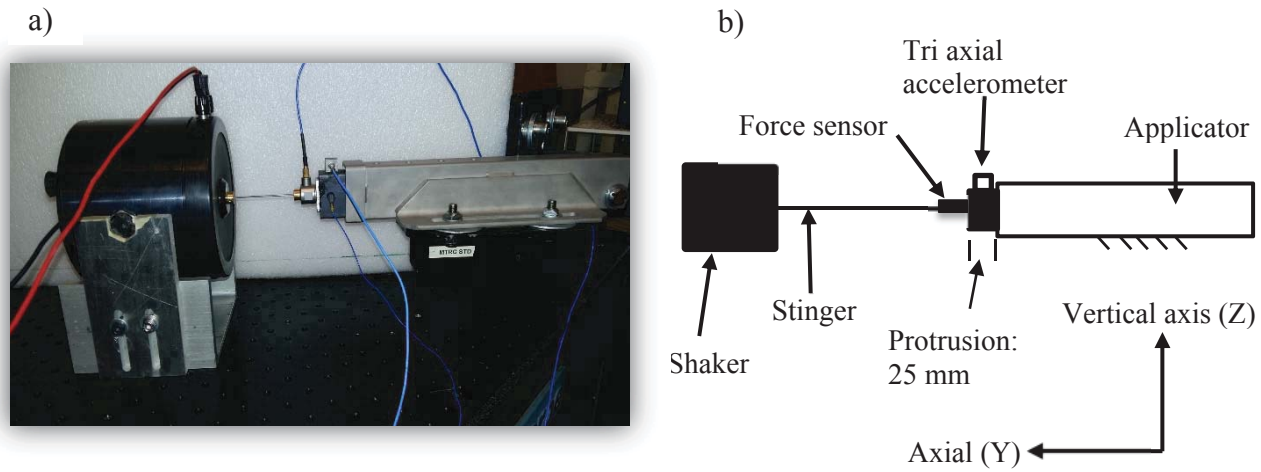

Figure 2.10 : Axial test of stick – applicator assembly, (a) experimental setup, (b) schematic of the axial test.

Experimentally measured accelerance (acceleration/input force) of stick-applicator assembly with two short interlocking sticks by using low-level sine-sweep excitation signal are shown in Figure 2.11.

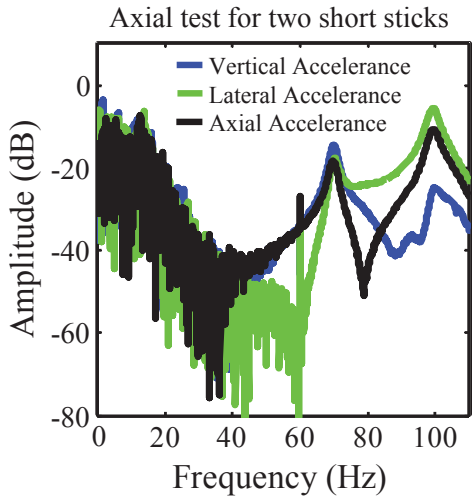

Figure 2.11 : Normalized response (acceleration) of the stick with respect to the force provided by the force transducer for stick-applicator assembly with two short sticks. Note that below 60 Hz, the response is noisy and low coherence was observed.

The same experiments with four short interlocking sticks and one long stick were conducted to see the effect of sticks on the linear behavior of the stick-applicator assembly. Extracted natural frequencies are summarized in Table 2.4.

Table 2.4 : Linear natural frequencies (Hz) of the stick-applicator assembly measured by the axial test

Modes (n)	1 long stick	2 short sticks	4 short sticks
1	69.97	68.90	68.29
2	99.43	98.36	97.06

It is deduced from the above that sticks marginally influence the linear natural frequencies of the stick-applicator assembly due to its mass and stiffness properties. Whereas it will be shown in section 2.2 that sticks can have important role to suppress the vibration and make a delay in

instability produced by stick-mock-wheel interaction. To get clearer view of the mode shapes of the results in Table 2.4, stick-insert assembly is studied experimentally and by using FEA in subsection 2.1.2.2.

2.1.2.2 Mode shapes of stick- insert assembly

To find the mode shapes associated with the natural frequencies measured by the axial test, insert was removed from the tube and it was clamped at one end. After that, two short interlocking sticks were connected to the insert by a tape. Figure 2.12 shows the experimental setup. Accelerance extracted by the impact hammer testing with the sensitivity of 11.2 mv/N are shown in Figure 2.13.

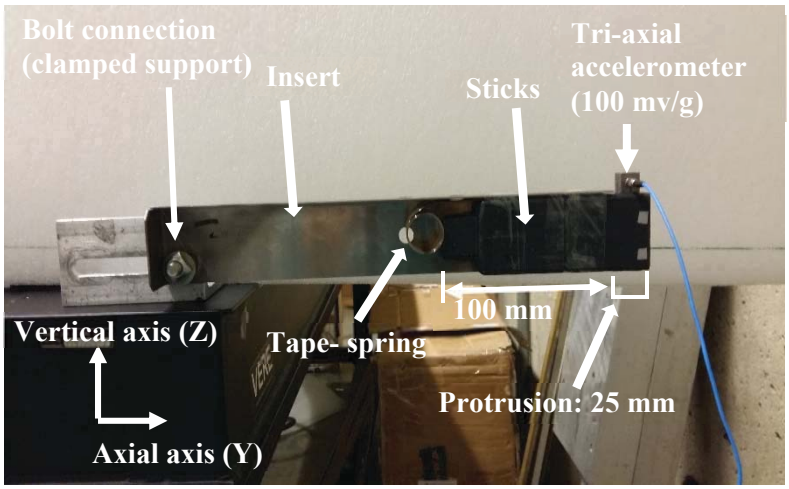

Figure 2.12 : Stick - insert assembly clamped at the end

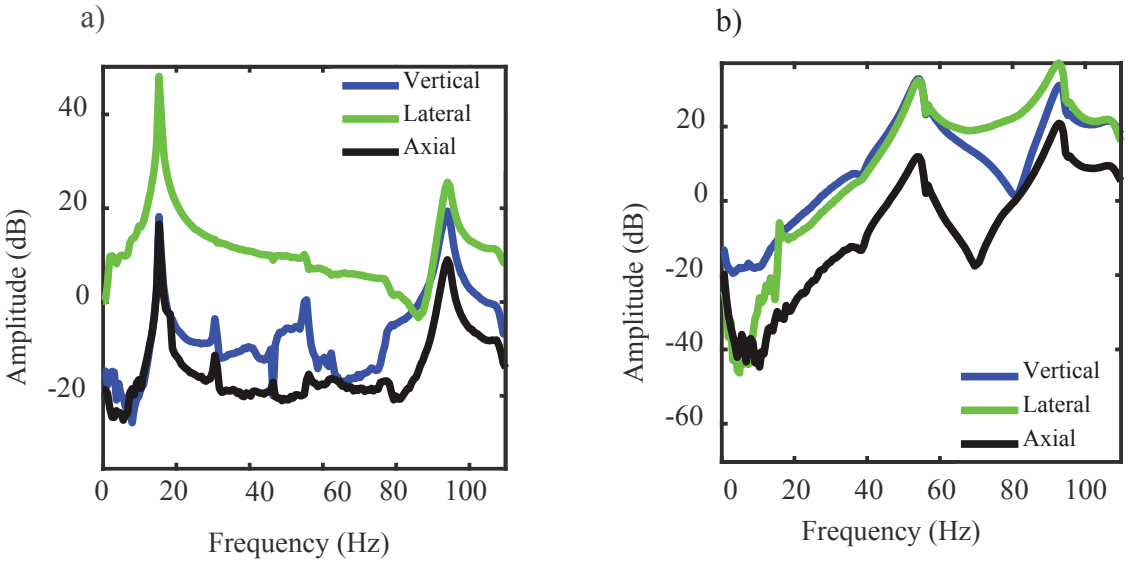

Figure 2.13 : Direct and cross accelerance of the stick - insert assembly clamped at the end; (a) lateral impact, (b) vertical impact

To verify the above experimental results, FE models of stick-insert assembly and insert alone (without considering the constant force spring) were made in ABAQUS. Shell elements were used to mesh the structure with thickness of 1mm and material properties such as 203 GPa as Young modulus, Poisson ratio of 0.265 and density of 7900 kg/m^3 . In stick-insert assembly, mode shapes based on treating the sticks as point masses are illustrated in Figure 2.14.

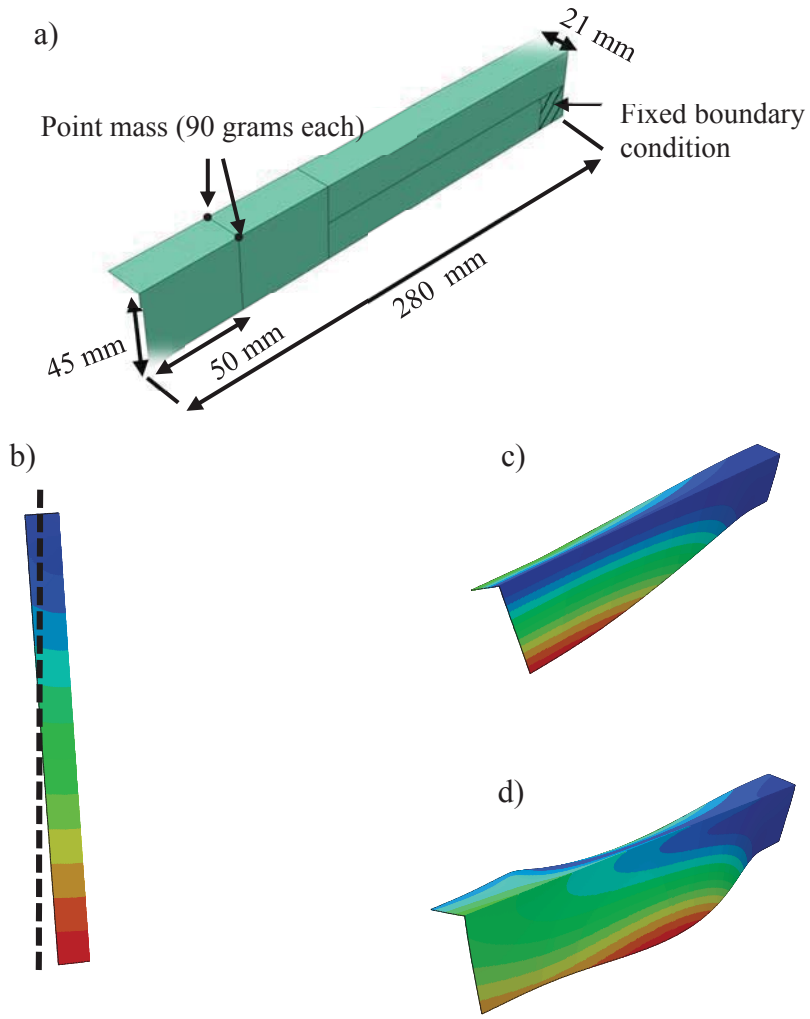

Figure 2.14 : (a) Stick-insert assembly with its geometrical properties in ABAQUS, (b) Top view of first mode (14.63 Hz), (c) second mode shape (54.02 Hz), (d) third mode shape (220.28 Hz)

Comparisons between the linear natural frequencies extracted by FEA analysis of stick-insert assembly, impulse test of stick-insert assembly and axial test of stick-applicator assembly with two short sticks are summarized in Table 2.5. Notice that insert's natural frequencies calculated by FEA and measured by experiments (impulse tests) are in good agreement. In addition, the first two modes computed by FEA for stick-insert assembly have been successfully verified by the impulse tests whereas a huge disparity exists between frequencies of the third modes. The difference might have to do with the fact that tape-spring interactions were not modelled in FE and sticks were simply treated as point masses. By comparing axial test results with impulse tests on stick-insert system, it is understood that the first mode around 70 Hz and the second mode around 100 Hz can be attributed to the second and third modes of stick-insert assembly respectively. The discrepancies in the results may be explained by virtue of the fact that when sticks and insert are placed inside the applicator, the applicator's wall adds more support to the stick-insert system along with varying the mass distribution of interlocking sticks. The first mode (around 15.5 Hz) in the stick-insert-assembly seems to be confined or not to be excited in the stick-applicator assembly.

Table 2.5 : Comparisons between the linear natural frequencies extracted by FEA analysis of stick-insert assembly, impulse test of stick-insert assembly, and axial test of stick-applicator assembly with two short sticks

Modes (n)	FEA		Impulse test		Axial test
	Stick-insert	insert	Stick-insert	insert	
1	14.63	28.6	15.5	27.7	69.97
2	54.02	110.57	56.94	108.03	99.42
3	220.28	282.28	92.28	273.10	--------

Identifying the linear characteristics of the stick-applicator assembly is a primary step in studying the nonlinear behavior of the system. Unfortunately, investigating the nonlinear behavior of the stick-applicator assembly was not possible through the axial test alone since increasing the axial excitation signal provided by the shaker, brings in shaker-stinger assembly dynamics.

Conducting other experiments to exactly characterize the nonlinear motion of stick-applicator assembly is postponed for future works (See chapter 4).

Having found the dynamics of each subsystem (i.e. mock-wheel and stick-applicator assembly), the next step is to study the case where mock-wheel is coupled to the stick-applicator assembly.

2.2 Stick- mock-wheel assembly (coupled system)

As mentioned before, the main purpose of this dissertation is to understand how stick- applicator assembly behaves during instability. Therefor, the lab-scale setup was designed for that purpose. Schematic of the set-up is given in Figure 2.15.

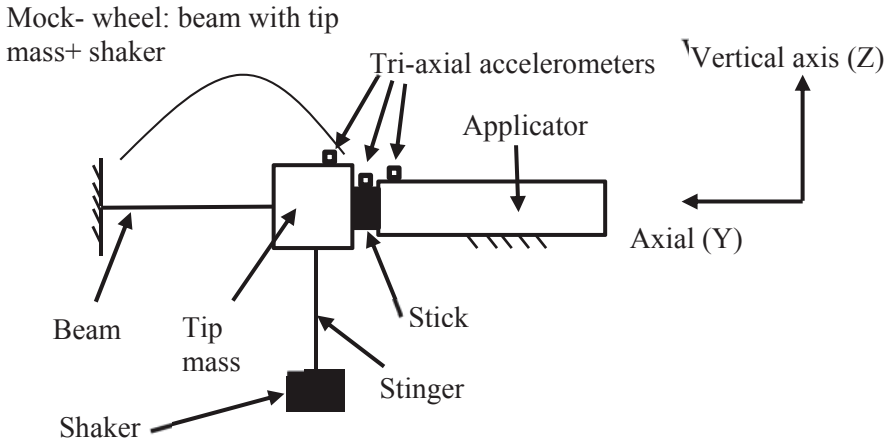

Figure 2.15 : Schematic of the lab-scale setup designed to examine the dynamics of stick- applicator assembly

Dynamics of each subsystem in Figure 2.15 (i.e. mock-wheel and stick-applicator assembly) was understood by various vibration testings described in previous sections. This section begins with identifying the linear modes of the coupled system. This is followed by studying how nonlinear motion evolves by increasing the excitation voltage fed by the shaker. The impacts of sticks and different insert's designs in suppressing the system's vibration are also addressed in this section.

2.2.1 Evolution of nonlinear motion from linear motion

Low-level sine sweep signal was used to identify the linear modes of the coupled system. When two short interlocking sticks were inside the applicator, the acceleration of the stick due to the swept-sine excitation was measured by the tri-axial accelerometer mounted on the stick. Figure 2.16 presents how the nonlinearities involved in the coupled system distort the linear natural modes of the coupled system with increasing the excitation level. It is evident that higher levels of excitation signal lead to softening behavior of the modes and resonance peaks may be flattened or sharpened. The observed softening behavior can be associated with mock-wheel's nonlinearities, interface nonlinearities due to contact and stick-applicator assembly nonlinearities such as gaps (clearances) between the stick and the applicator. Similar trend and natural frequencies were observed by acceleration measured on the mock-wheel but are not shown here. It should be pointed out that the first two modes found in the coupled system subject to low level of excitation voltages are close to ones demonstrated by the axial test. For high level of excitation voltages and the frequencies less than 70 Hz (first mode of the stick-applicator assembly), nonlinear resonances may govern the dynamics of the coupled system. Linear natural frequencies of the coupled system for different conditions are tabulated in Table 2.6. slight differences in linear modes were achieved by changing type and number of sticks inside the applicator.

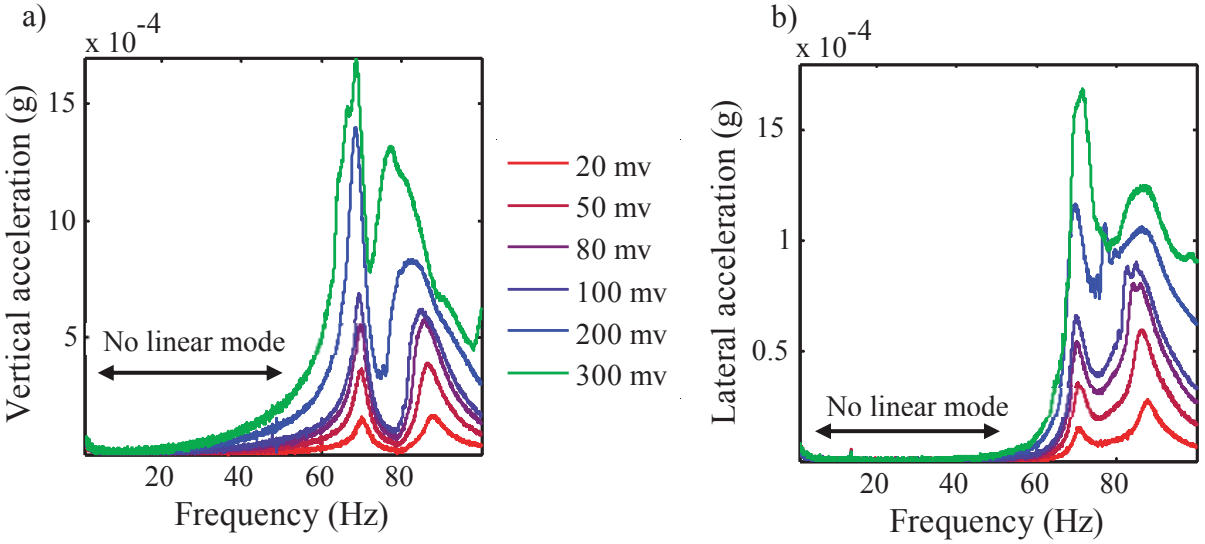

Figure 2.16 : Experimental frequency spectrum of the stick in the coupled system with increasing excitation level (from20 mv to 300 mv); (a) vertical acceleration of the stick, (b) lateral acceleration of the stick

Table 2.6: Linear natural frequencies (Hz) of the coupled system with different type and number of sticks inside the applicator.

Modes (n)	1 long stick	2 short sticks	4 short sticks
1	71.50	71.22	69.67
2	87.85	90.83	78.18

The appearance of nonlinear resonances, which generally depend on the external frequencies applied on the structure and excitation amplitude, between 10 to 60 Hz by increasing the excitation voltage of the swept-sine signal is depicted in Figure 2.17. Time is converted to sweep frequency according to the sweep rate.

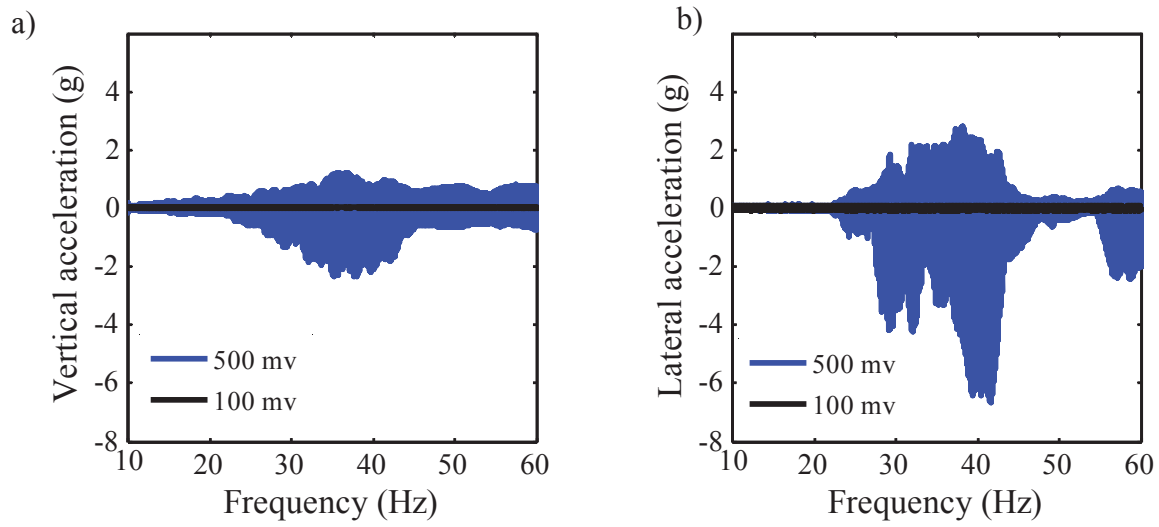

Figure 2.17 : Appearance of nonlinear resonances between 10 to 60 Hz by increasing the excitation voltage of the swept-sine signal in the coupled system with two short sticks; (a) vertical acceleration of the stick, (b) lateral acceleration of the stick

Observing noticeable vibration in the range of 20 to 50 Hz, which can be associated with the presence of nonlinear resonances appearing by higher excitation amplitudes, was a motivation to investigate each integer frequency below 60 Hz leading to the construction of experimental stability plot.

2.2.1.1 Experimental stability plots

Experimental stability plot for the coupled system including two short sticks inside the applicator is shown in Figure (2.18). The response of the coupled system at 37 Hz, as an example, is studied here.

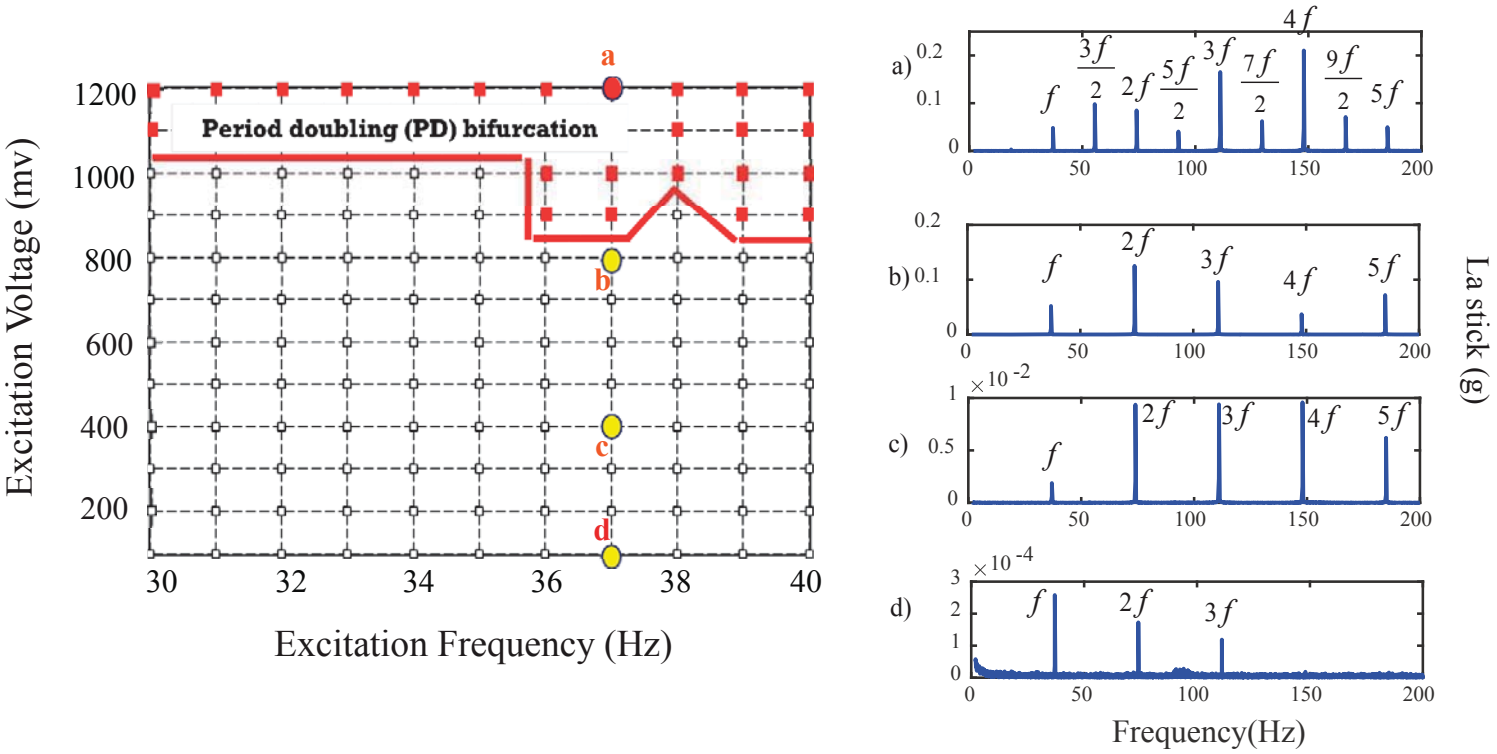

Figure 2.18 : Experimental stabilit y plot for the coupled system including two short sticks inside the applicator. 37 Hz is chosen as an example to demonstrate the lateral nonlinear motion of the system. La stick stands for lateral acceleration of the stick. FFT of the stick lateral acceleration at (a) 1200 mv, (b) 800 mv, (c) 400 mv and (d) 100 mv excitation voltage.

Each frequency was tested by a harmonic excitation at different amplitudes to see the evolution of nonlinear response and occurrence of instability in the coupled system. It is worth mentioning that less than 100 mv of excitation amplitude and in the frequency range less than 50 Hz, system behaves linearly. Period-doubling bifurcation was observed as an instability in the range of frequencies and amplitudes depicted in the above stability plot. The maximum achievable excitation voltage was 1.2 volts due to shaker operating conditions.

Onset of period-doubling bifurcation is identified both by sonogram (Short Time Fourier Transform or STFT) analysis of the results of the sweep amplitude excitation signal with excitation frequency of 37 Hz and observation of a jump in stick's lateral Rms values caused by motion transfer from the mock-wheel to the stick (Figure 2.19).

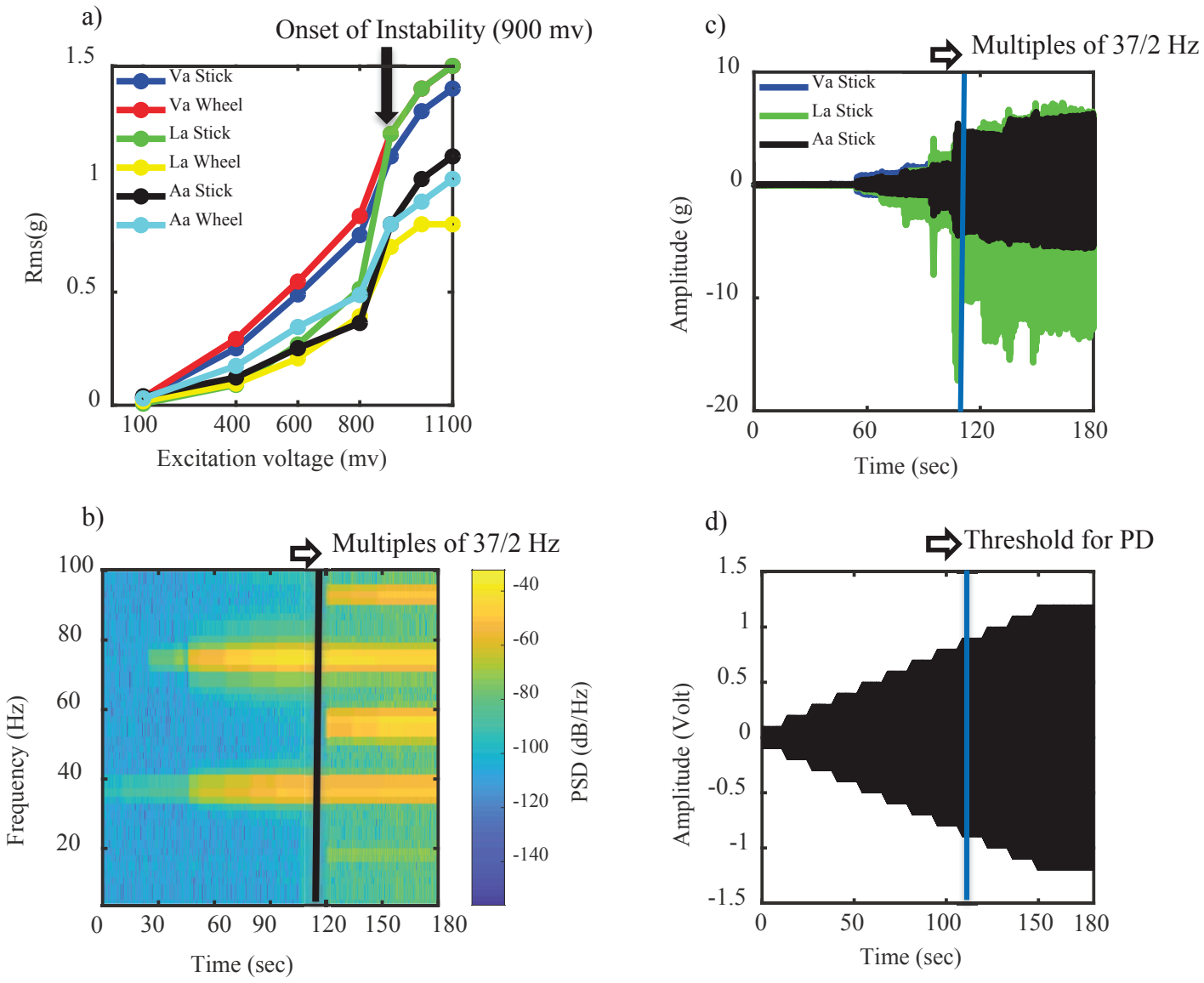

Figure 2.19 : Verification of the onset of PD at excitation frequency of 37 Hz for the coupled system comprised of two short interlocking sticks; (a) Rms values at different separate excitation amplitudes, (b) lateral acceleration of stick at 37 Hz excitation frequency and sweep amplitude signal, (c) stick's acceleration in time domain due to sweep amplitude signal, (d) sweep amplitude signal.

As shown in figure 2.17, increase in the excitation amplitude resulted in the appearance of nonlinear resonances between 30 to 40 Hz both in vertical and lateral direction of the coupled system. It is also evident from the stability plots that the threshold of the excitation voltage for the frequencies of 36, 37, 39 Hz above which vertical motion transfers to lateral motion accompanied by jump and PD bifurcation is lower than the rest of the frequencies. Essentially, it can be hypothesized that one to one internal resonance between vertical direction and lateral direction exists in the coupled system. To check this hypothesis, scanning Vibrometer (PSV 400) was also used to measure the lateral response (displacement and velocity) on both the stick and the mock-wheel of the coupled system during PD bifurcation (Figure 2.20). Since the same trend was observed in mock-wheel's lateral motion, only the frequency spectrums of displacement and velocity measured on the lateral side of the stick is illustrated in Figure 2.21. It is clear that when the coupled system is excited at 37 Hz and 1.2 volts, PD occurs and 37 Hz is the dominant peak in the response. That manifests the possibility of having a (nonlinear) mode in the vicinity of 37 Hz in the lateral direction which is coupled to a vertical (nonlinear) mode around 37 Hz through nonlinearities. When PD occurs, that (nonlinear) lateral mode at 37 Hz becomes unstable. Observation of other harmonics in the response is associated with several odd and even nonlinearities .

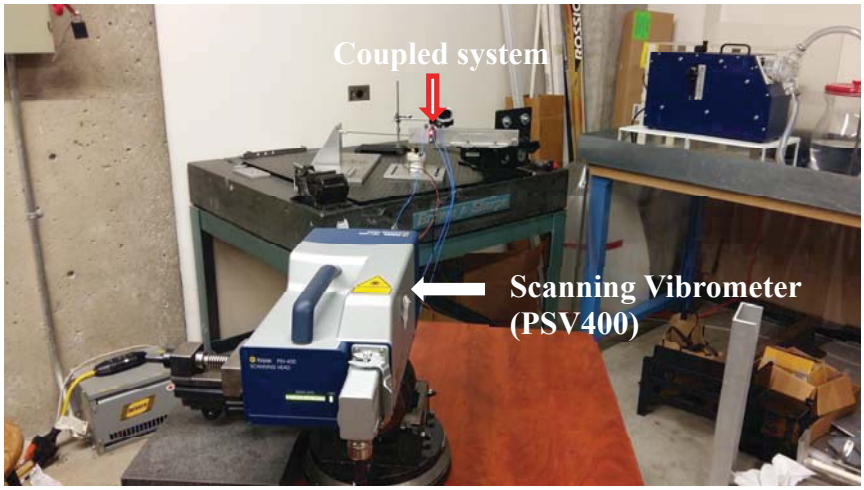

Figure 2.20 : Measuring displacement and velocity of the lateral motion by the scanning Vibrometer (PSV 400)

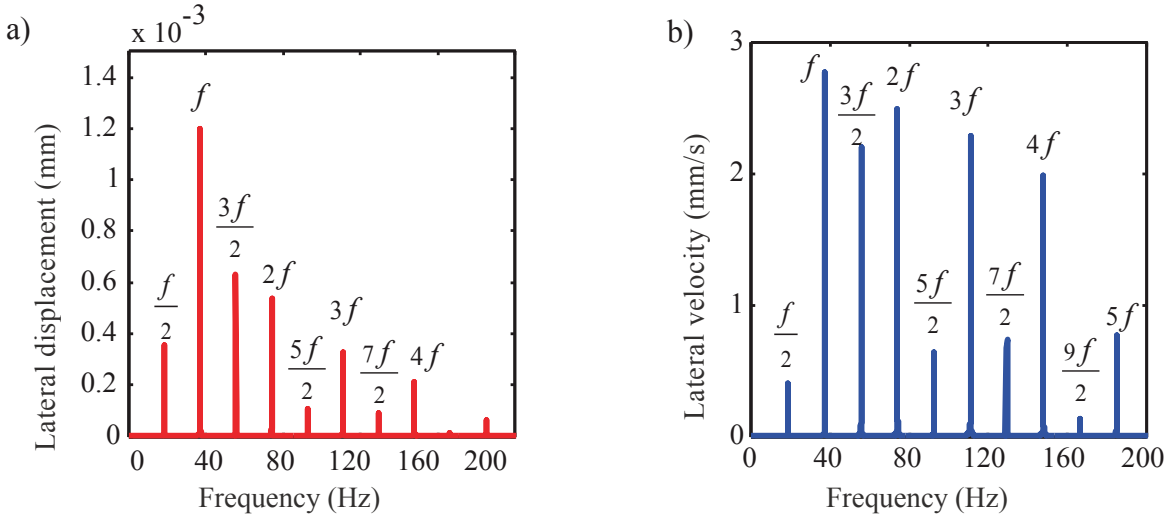

Figure 2.21: Frequency spectrum of the lateral response measured on the stick due to the excitation voltage and frequency of 1200 mv and 37 Hz; (a) lateral displacement, (b) lateral velocity

assuming that the lateral nonlinear mode around 37 Hz becomes unstable for higher excitation voltages, it is reasonable to recognize the lateral stiffness as one of the significant design parameters in the coupled system and identify the practical ways such as modifying the parts used in stick-applicator assembly to increase the lateral stiffness in the coupled structure. To this end , it was shown that introducing external lateral supports with foam at tip connected to the protruded stick is capable of eliminating instability and decreasing the vibration level in the structure noticeably (Figure 2.22 and Figure 2.23).

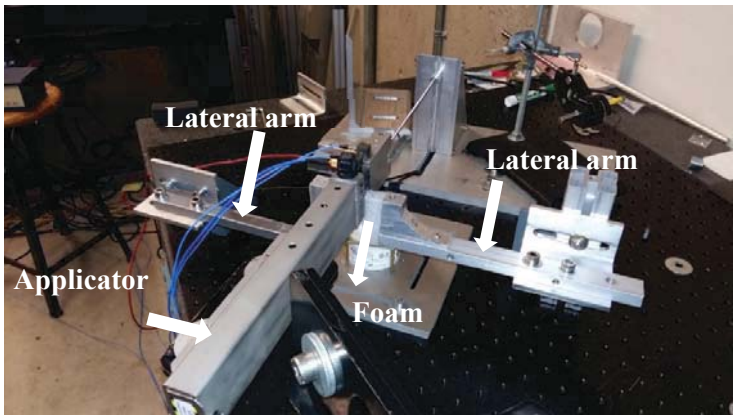

Figure 2.22 : Experimental setup utilizing external lateral supports connected to the stick

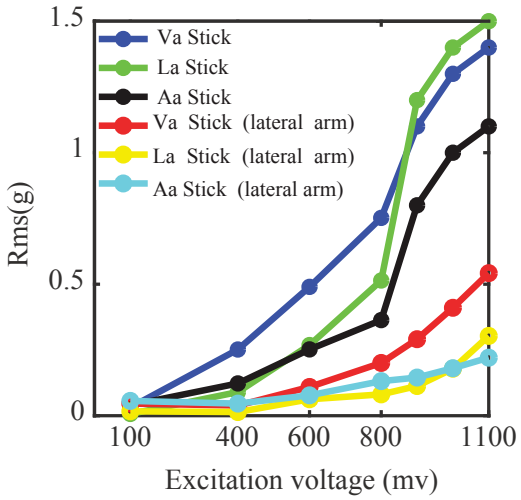

Figure 2.23: Comparisons between Rms values of the coupled system having two short sticks with and without adding external lateral supports

Having recognized the parameters controlling instability in the coupled system such as excitation voltage and frequency to produce consistent instability in the coupled system , the remaining issue about the lab-scale setup is how to suppress the vibration and eliminate instability by modifying the parts such as sticks and insert used in stick-applicator assembly. It is trivial that changing the mock-wheels' design parameters can also suppress the vibration but that is not what this project looks for. In reality, when stick-applicator is in contact with the real train wheel, the pertinent and available parts dealing with vibration reduction are sticks, insert, applicator and bracket. Due to safety issues, it is not possible to add external lateral supports inspired by the experiment explained in Figure 2.22. Next subsections discuss the influence of sticks and insert on lowering the vibration in stick-applicator assembly by increasing the lateral stiffness.

2.3 Vibration reduction in stick-applicator assembly

Earlier in chapter 1, it was mentioned that applicators are prone to failure because of the motion transfer from the sticks inducing fatigue-related problems through vibro-impact mechanism. However, suspension (bracket) motion of the stick-applicator assembly is important as well which is out of the scope of this work. The vibration level (Rms (g)) of the tube in the stick-applicator assembly including two short sticks coupled with the mock wheel excited at 37 Hz with different

excitation amplitudes is given in Figure (2.24). It is clear that portion of the stick motion is transferred to the applicator. Moreover, vibro-impact phenomenon was observed to exist by roving a microphone around the coupled system. It was found that the noise coming from the stick-applicator interaction is stronger than the one originating from the stick-mock wheel interaction (Figure 2.25).

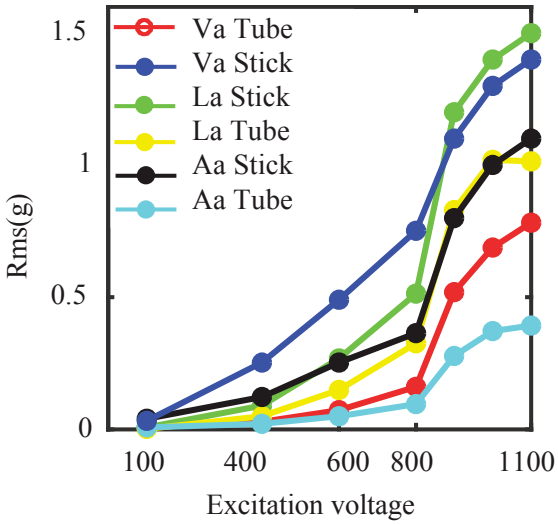

Figure 2.24: comparing the Rms values of stick and applicator (tube) at 37 Hz and different excitation levels

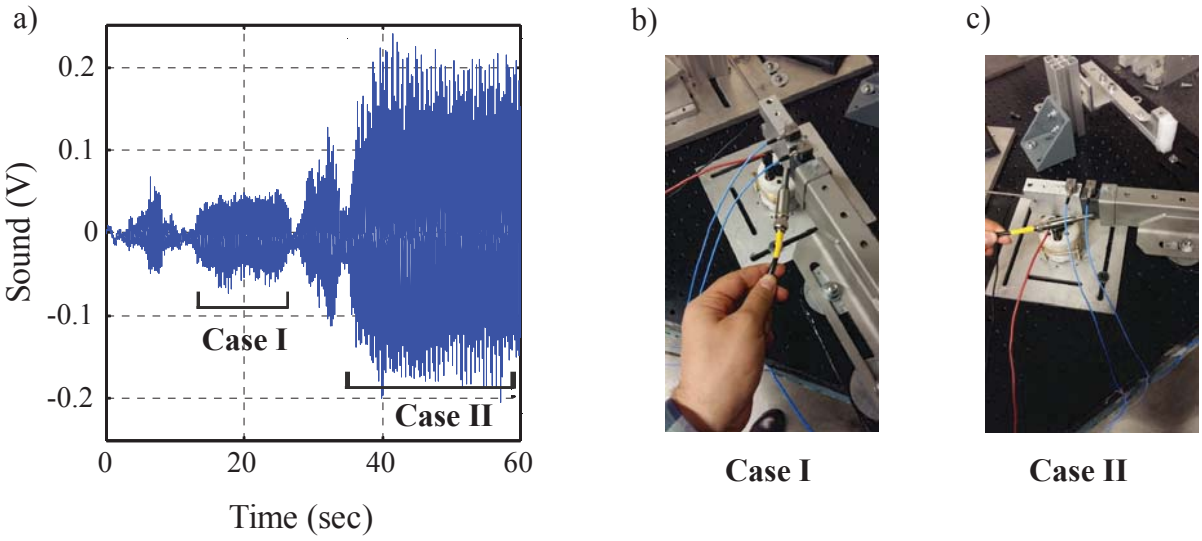

Figure 2.25 : Vibro-impact phenomenon by roving the microphone around the coupled system; (a) noise signal during system's operation at high excitation voltages; (b) microphone close to the stick-mock wheel interface, (c) microphone close to the entrance of the applicator

As suggested earlier in Figure 2.22, increasing lateral stiffness in the coupled system lowers vibration. It was also pointed out that sticks, insert, applicator (tube) and the bracket are the most accessible parts to be considered for decreasing the vibration level in the coupled system. In the following subsections , the effect of sticks and insert are studied and it is described how sticks design and insert's design can contribute in enhancing the lateral stiffness in the coupled system.

2.3.1 Stick's impacts on vibration suppression

The stability of the coupled system including two short interlocking sticks inside the applicator was already studied. It has been shown that PD bifurcation occurrence depends on both excitation frequency and amplitude. Two further cases are given attention in this subsection to see how the nonlinear motion of the coupled system alters. From the linear tests, it was demonstrated that having four short interlocking sticks or one long stick inside the applicator could not change the first two linear modes of the coupled system significantly (Table 2.6). Nonlinear vibration tests (i.e. having constant excitation frequency and various excitation amplitudes up to 1.2 volts) help to understand the role of sticks in suppressing the vibration. In this regard, response of the coupled system incorporating two short interlocking sticks, 4 short interlocking sticks and 1 long stick excited at 37 Hz and different excitation amplitudes are plotted in Figure 2.26. It is evident that the more interlocking sticks inside the applicator, the higher the level of vibration is. In addition, the required threshold of excitation voltage for PD bifurcation has dropped from 900 mv (for two short sticks) to 500 mv (for four short sticks). The other interesting thing is intermittency in PD bifurcation for four short sticks as can be seen in Figure 2.26 (b). That needs to be studied in future studies to get clearer understanding of the stick-applicator interaction. It is also clear that using one long stick causes less vibration level and elimination of PD bifurcation. When 1 long stick was inside the tube, other frequencies less than 60 Hz were also checked and PD bifurcation was not observed by increasing the excitation voltage up to 1.2 volts. Elimination of PD bifurcation in the coupled system by using 1 long stick instead of two short interlocking sticks may have to do with the fact that the presence of looseness between two interlocking sticks undermine the lateral

stiffness provided by the sticks. Therefore, proper stick's designs are crucial for having less vibration in the stick-applicator assembly.

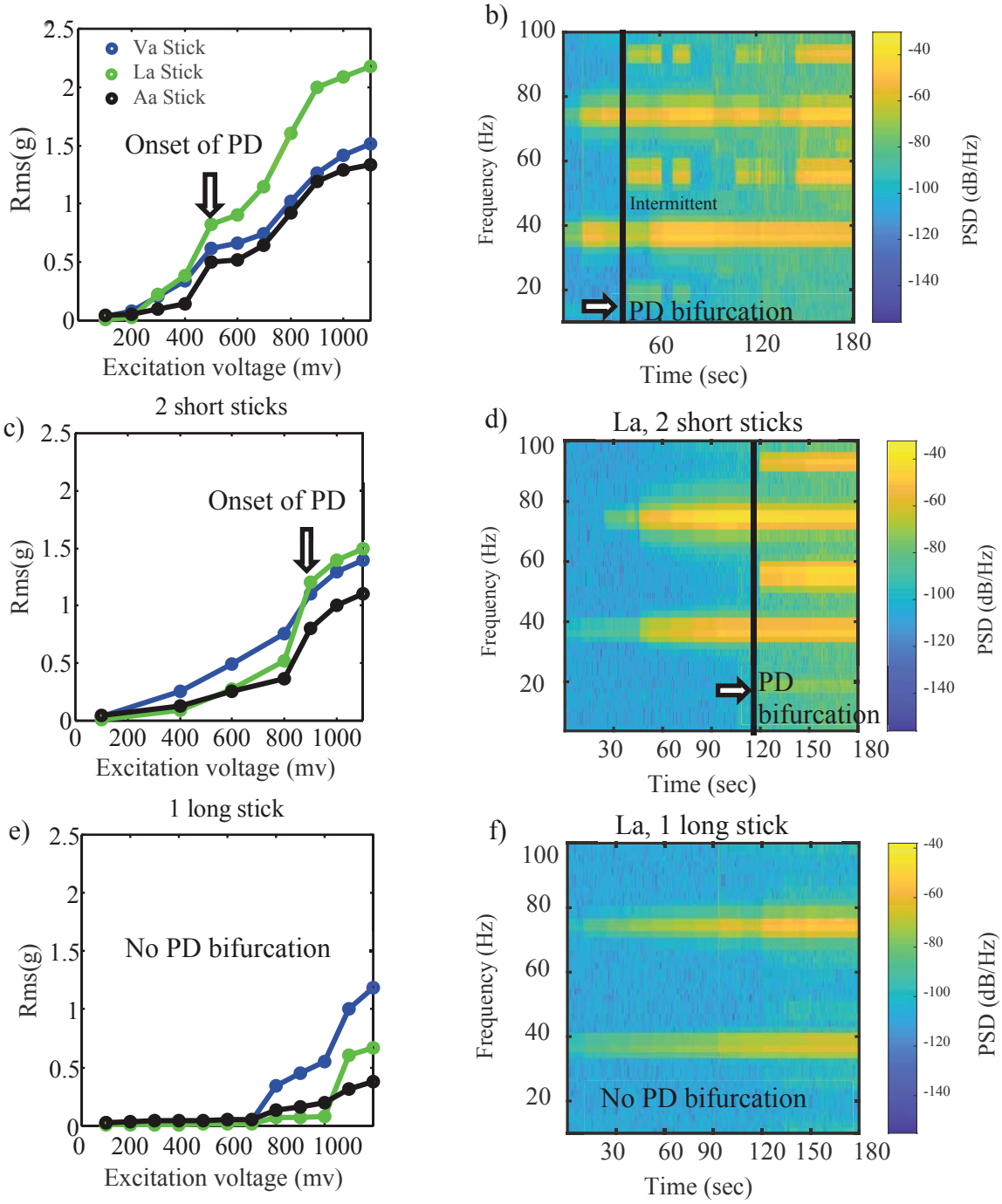

Figure 2.26 : Rms values of (a) 4 short sticks (c) 2 short sticks (e) 1 long stick at 37 Hz excitation frequency and different separate amplitudes; STFT of lateral acceleration of (b) 4 short sticks (d) 2 short sticks (f) 1long stick at 37 Hz excitation frequency and continuously varying amplitude

2.3.2 Insert's impacts on vibration suppression

Insert also has contribution in providing lateral stiffness in the coupled system. As mentioned earlier, clearances exist in stick-applicator assembly due to manufacturing process. The loose connection between the sticks and insert prevents the insert to be efficient in providing lateral stiffness in the coupled system. To overcome the aforementioned issue, insert's designs are important. It is noteworthy to mention that insert can be treated as a passive compensator for the applicator (tube), so it is possible to reduce the tube's vibration originating from stick motion by compensating the insert. Two insert's designs named regular insert and regular curved insert (known as damped insert in industry) have been used earlier but they were not successful in reducing the vibration and noise level emanated by stick-train wheel interaction. Note that the measurements presented so far were for stick-applicator assembly with regular insert only. Having identified the role of lateral stiffness in the present lab-scale setup at UBC, two more insert's designs called short-bend insert and top-bend insert were asked to be made to investigate the efficacy of insert designs in decreasing the vibration level in the lab-scale setup. The schematic of four different insert designs is illustrated in Figure 2.27.

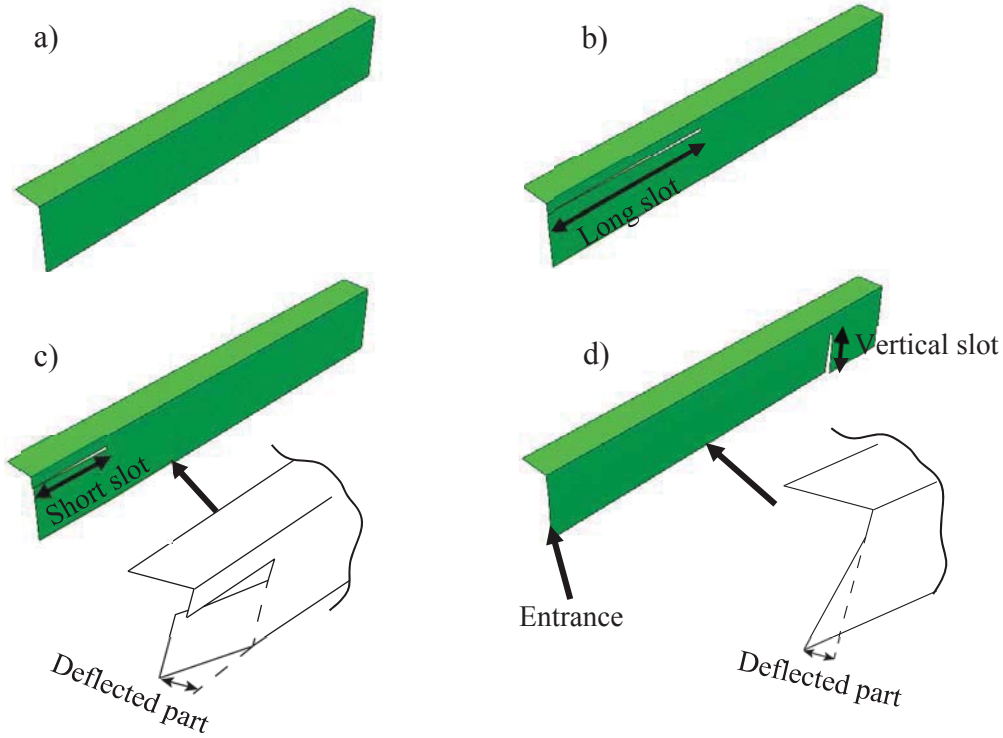

Figure 2.27 : (a) Regular insert, (b) Regular curved insert, (c) Short bend insert, (d) Top-bend insert

The main idea behind new insert designs is to increase lateral stiffness in the coupled system by reducing the gap between sticks and insert. Interaction between sticks and insert can be treated as a nonlinear joint due to the presence of the free-play. As shown in Figure 2.28, by assuming sticks, insert and applicator as a discrete mass, springs and rigid stops respectively, stiffness discontinuity may exist due to the presence of the clearances in the stick-applicator assembly. The presence of discontinuity in the system's parameter can be the cause of nonlinear behaviors such as period-doubling bifurcation and chaotic motion [29,37,44,45]. Therefore, eliminating the gaps in the stick-applicator assembly could help eliminate the PD bifurcation and decrease the motion transfer from the sticks to the applicator.

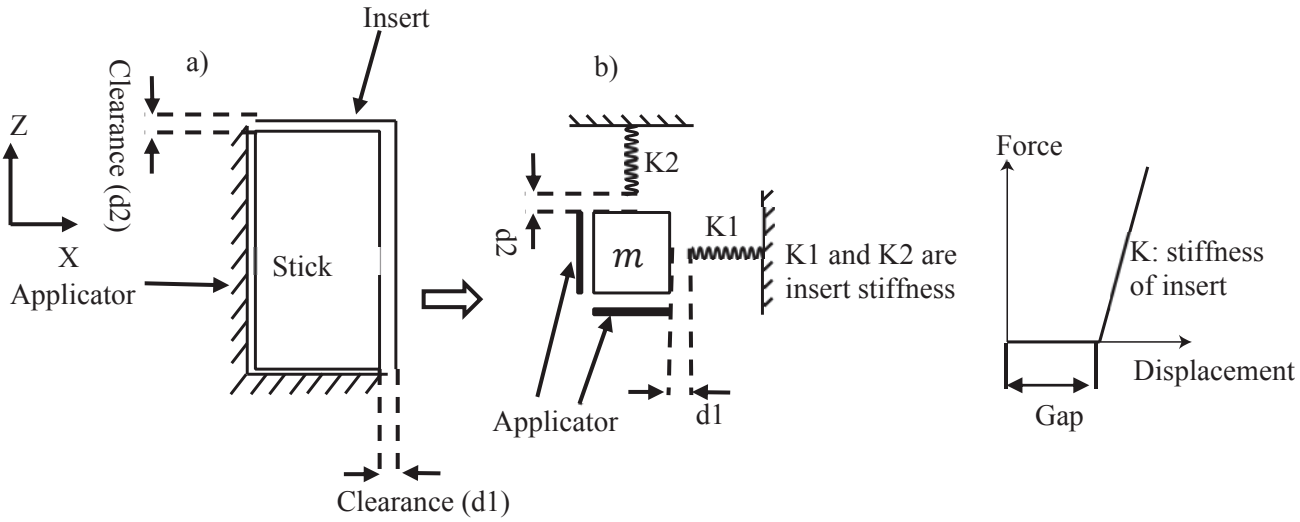

Figure 2.28 : a) Front view of the stick-applicator assembly, b) qualitative model of stick-applicator assembly showing clearances and stiffness discontinuity

In that regard, a horizontal slot is created in the side wall of both short bend and regular curved insert and based on the length of the slot, the lower section is deflected (Figure 2.27 (c)). That deflected part fills the gap between the stick and insert in the entrance of the applicator. In top-bend insert, a vertical slot near the end of the insert is first created and a certain deflection is given to the section from the entrance to the slot (Figure 2.27 (d)) making the insert in contact with stick s through a line. Inserts are made of the same material.

Static stiffness analysis as an approximate method for the first mode can be used to compare the stiffness of each insert without sticks. To this end, the inserts were modelled in ABAQUS and two different loading conditions were assumed (Figure 2.29). In this analysis, static stiffness is defined as the ratio of the total applied force to the deflection of a (red) point in the middle of the sidewall of the inserts' entrance. Damping ratio of the inserts for the first mode were also measured by the modal experiments similar to what has been done earlier in Figure 2.10. It was found that damping ratio for the inserts are almost constant.

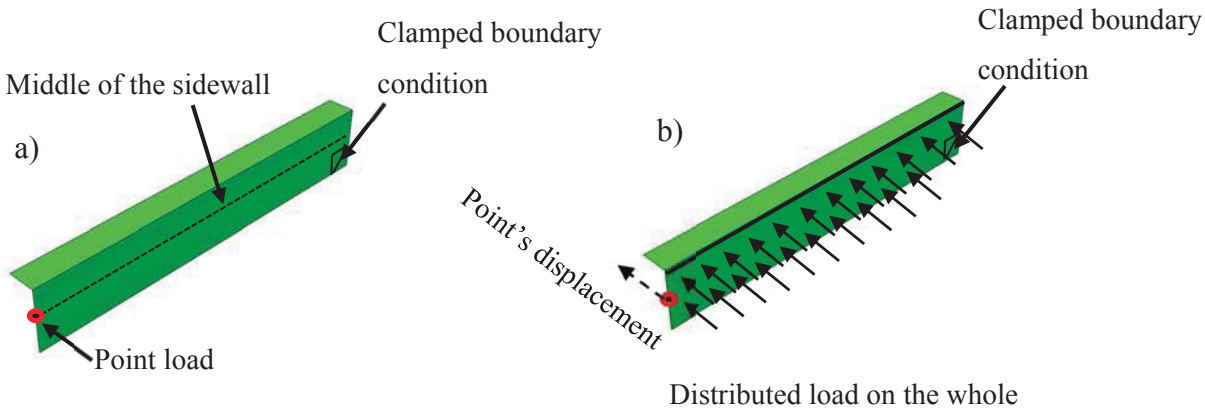

Figure 2.29 : (a) Insert under a point load applied at the entrance, (b) Insert under a distributed load applied on the sidewall

Table 2.7 represents the damping ratio and normalized static stiffness with respect to the stiffness of the regular insert . It is observable that the regular insert has the highest lateral static stiffness but the presence of gap between the sticks and insert reduces the efficacy of the regular insert.

Table 2.7 : Comparison of static stiffness and damping ratio for different inserts

	Regular insert	Regular curved insert	Top -bend insert	Short -bend insert
Normalized static stiffness				
Point load	1	0.435	0.8718	0.8820
Distributed load	1	0.6858	0.9016	1.02
Damping ratio	0.011	0.0164	0.0124	0.0105

Regular insert was replaced by the other three inserts to see whether instability occurs or not when two short sticks are inside the tube. PD was not observed during the operation of the other inserts in the operating frequency range of 5 to 60 Hz. Figure 2.30 shows the Rms values of the coupled system including two short interlocking sticks and different inserts. Vibration reduction of sticks caused by top-bend insert and short bend insert is noticeable compared with regular curved insert and regular insert. Once the stick's vibration was suppressed the vibration of the coupled system decreased because of providing lateral stiffness to the structure.

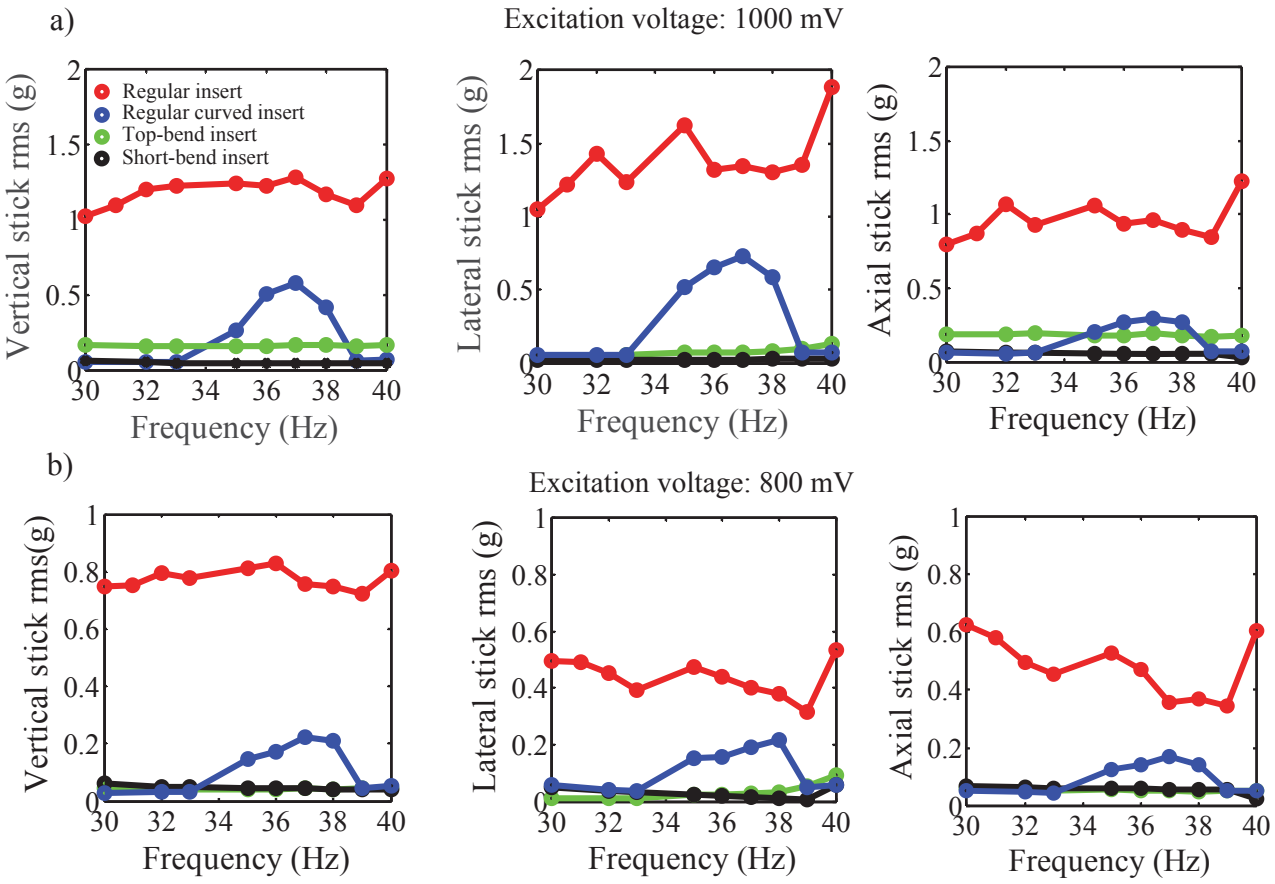

Figure 2.30 : Evaluating the inserts' performance in terms suppressing the stick's vibration level ; (a) Rms values of vertical, lateral and axial acceleration of the stick due to various excitation frequencies and constant excitation amplitude of 1000 mv,(b) Rms values of vertical, lateral and axial acceleration of the stick due to various excitation frequencies and constant excitation amplitude of 800 mv

It can be deduced from the above figures that filling the gaps between the sticks and insert can result in having effective lateral stiffness provided by the insert in the coupled system and less vibration of sticks/applicator. The efficacy of different insert designs in the full-wheel test rig system is discussed in the next chapter.

2.3.3 Conclusion

This chapter was concerned with identifying the dynamics of the lab-scale setup and recognizing the practical and accessible ways to suppress the vibration in stick-applicator assembly. To better understand the dynamics of the coupled system, each subsystem dynamics was studied. It was shown that both mock-wheel and stick-applicator assembly are nonlinear systems and when these two subsystems were coupled to each other, interesting nonlinear behaviors such as internal resonance and period doubling bifurcation might occur. Having produced a consistent instability in the coupled system in certain excitation frequencies and amplitudes, the role of stick designs and insert designs were given attention to suppress the vibration level and eliminate the instability. It was shown that looseness between interlocking sticks and clearance between the sticks and the insert are significant parameters for preventing instability and the fatigue-related problems in the stick-applicator assembly. To that end, new inserts were designed to act as passive compensators to suppress the stick motion and consequently tube's vibration. The effectiveness of different insert designs in the full-wheel test rig system is discussed in the next chapter.

Chapter 3: Full-wheel rig experiments

3.1 Introduction

It was explained in the last chapter that modifications in insert designs to fill the gap between the stick and the applicator were effective in reducing vibration of stick-applicator assembly in the lab-scale setup. Lab-scale setup was designed to produce consistent instability in a controllable condition. Furthermore, lab-scale setup helped the study of stick-applicator assembly behavior during instability. However, some limitations exist in the lab-scale setup which are not present in the Full-wheel test rig (FWTR). First of all, the amount of input energy provided by the mock-wheel is less than the one afforded by the wheel in FWTR. Therefore, nonlinearities in the stick-applicator assembly in FWTR can be more intensified. Intensification of nonlinearities may lead to complex nonlinear behaviors. FWTR includes rotational motion of the wheel, which is the dominant motion, and unsubstantial reciprocal motion due to slight misalignments in the wheel and rotor connections. Whereas, lab-scale setup was targeted to provide reciprocal motion. Sticks are in contact with the wheel flange in field experiments. Flange effects were neglected in the lab-scale setup. Due to higher relative motion present in the stick-wheel interaction of FWTR, sticks get worn faster. Both the stick profile at the sliding interface and material of the tip mass used in the lab-scale setup differ from the FWTR. Thereby, contact properties of FWTR is more complicated than the lab-scale setup.

Considering the aforementioned restrictions on the lab-scale setup, FWTR experiments are carried out to evaluate the effectiveness of the insert designs in suppressing the vibration level in stick-applicator assembly. Figure 3.1 presents the test rig designed to investigate applicator-train wheel interaction using a freight wheel and without considering the rail-wheel interaction. Two tri-axial accelerometers are used to measure the acceleration of the stick and the applicator (Figure 3.1 (b)) during the operational tests. Proximity sensor is also used to measure the wheel runout which was found to be negligible. The maximum speed provided by the driving motor is 600 rpm. Four short interlocking sticks were placed inside the applicator and four different inserts, which were introduced in section 2.3.2, were tested accordingly at different wheel speeds.

a) b)

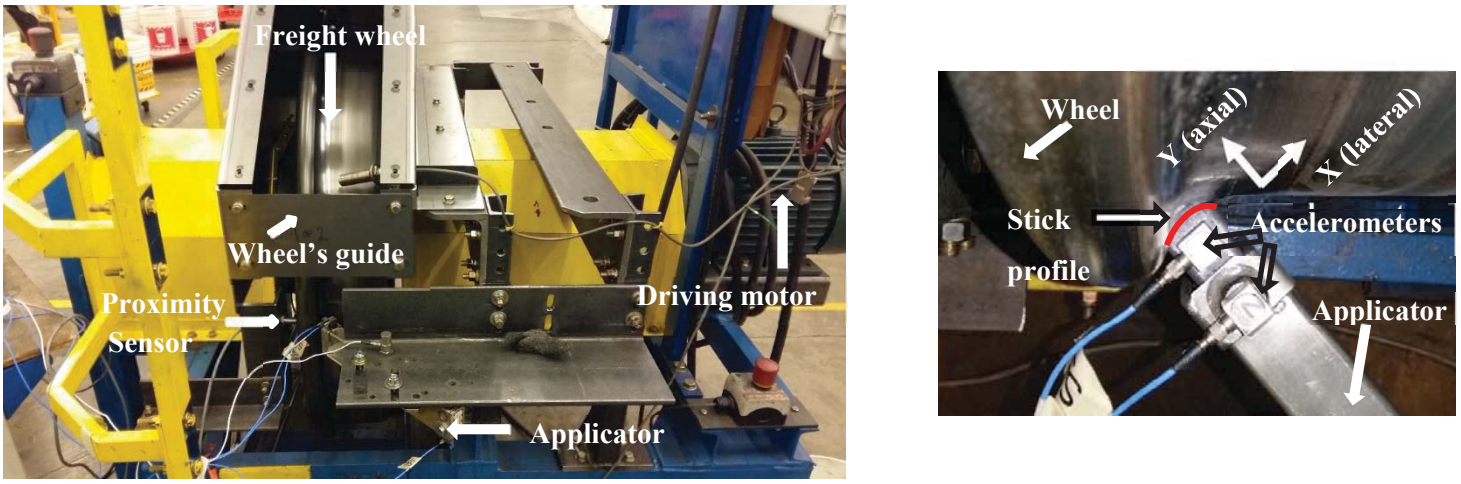

Figure 3.1: Full-wheel test rig experiment using freight wheel; (a) general view of the setup, (b) top view of the wheel's flange and stick-applicator assembly

3.2 Experimental results

It was noticed that lower wheel speed (less than 10 rpm) produces instabilities and gradual growth in the response of the stick-applicator assembly. However, most of the vibration in the FWTR setup is a stable forced vibration. In reality, wheel operates higher than 10 rpm, therefore having instabilities in lower speeds is not as important as the fatigue-related issues of forced vibration in the higher speeds.

Studying the response of the stick-applicator assembly in lower speeds can be helpful to gain an insight of the contributing factors in the dynamics of the coupled system. To achieve that, the responses of the stick-applicator assembly with regular-insert and top-bend insert in contact with the freight wheel are depicted in Figure 3.2 and Figure 3.3 respectively for wheel speed of 10 rpm. Figure 3.2 and Figure 3.3 show representatives record of friction-induced vibration. As shown in Figure 3.2 (a), instability occurs several times within 30 seconds. Figure 3.2 (b) demonstrates portion of the response which includes the vibration initiation (rapid growth), bounded vibration and gradual decay. Figure 3.2 (c) illustrates a dominant peak at 847.5 Hz. It can be a representative of a mode of the structure around 850 Hz becoming unstable due to certain conditions provided by the frictional contact. Furthermore, attachment and detachment status were observed between stick

and wheel flange. Attachment status was in coincidence with the rapid growth in response and annoying noise which are the indications of an unstable oscillation [7, 11,46]. Contact properties at the stick-wheel interface and the mechanism of instability (i.e. mode coupling, stick-slip, etc.) need to be carefully investigated by future studies.

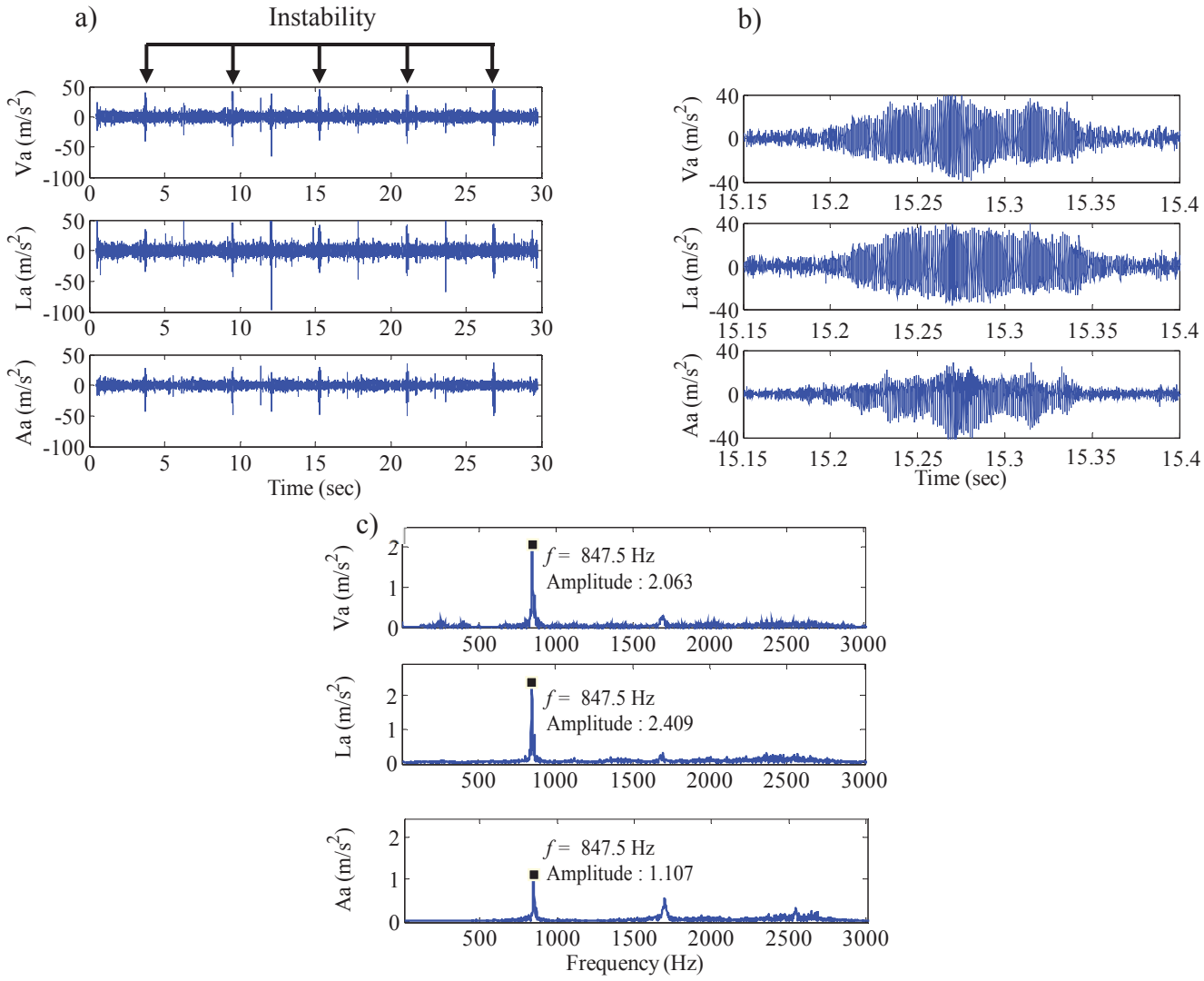

Figure 3.2: Stick acceleration at 10 rpm and regular insert in use; (a) total measurement, (b) rapid growth in the response (occurrence of instability), (c) FFT of response in b

Using top-bend insert led to an unstable oscillation with the dominant frequency of 397 Hz (Figure 3.3 (c)) in vertical direction. Figure 3.3 (a) depicts instabilities within 30 seconds. Figure

3.3 (b) demonstrates portion of the response which includes the vibration initiation (rapid growth), bounded vibration and gradual decay.

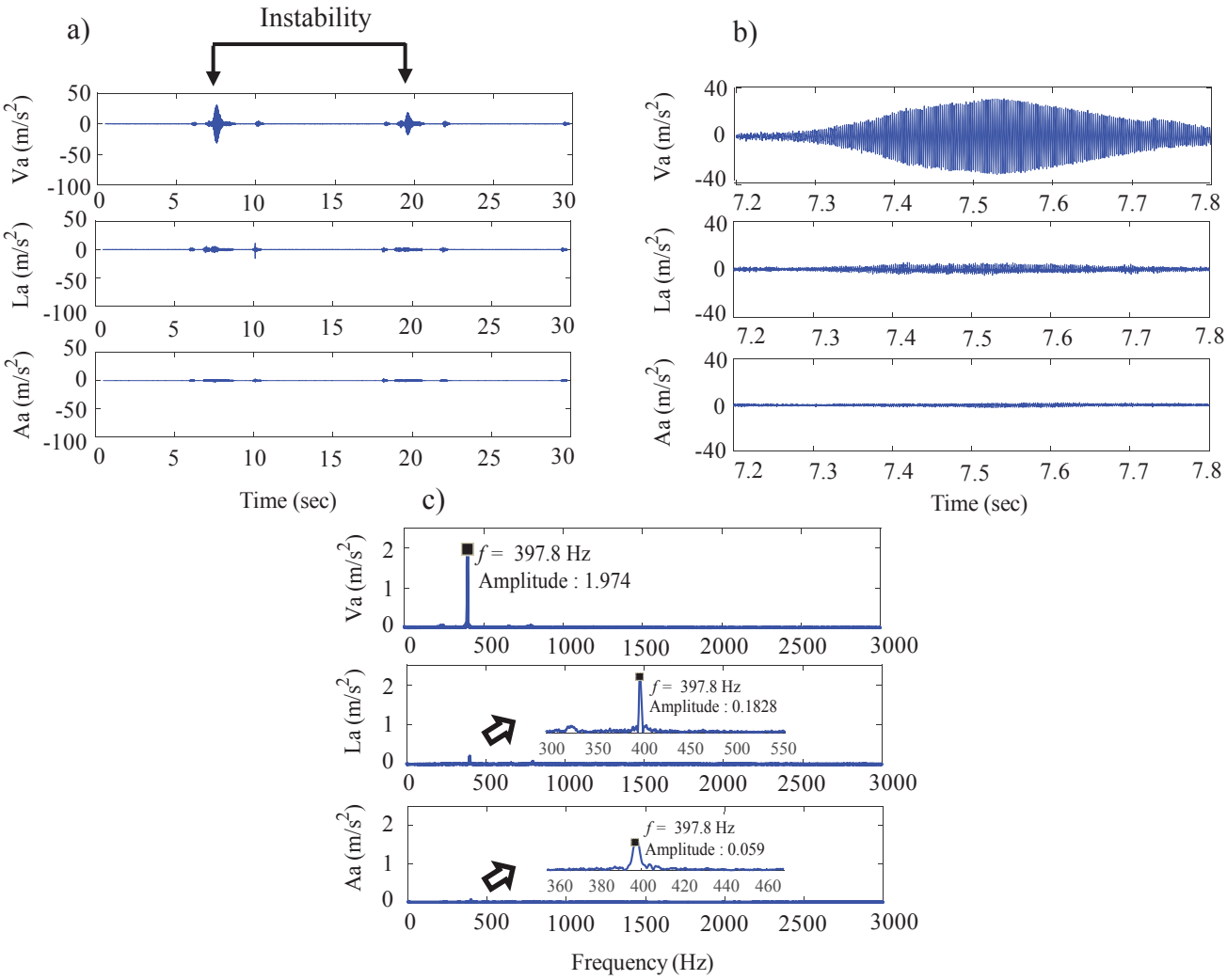

Figure 3.3 : Stick acceleration at 10 rpm and top-bend insert in use; (a) total measurement, (b) rapid growth in the response (occurrence of instability), (c) FFT of response in b

Two other inserts (i.e. short-bend insert and regular curved insert) were also tested in lower speeds. The data pertaining to these tests are not shown in this section since repeatability was not observed in the response.

Based on the above results, it can be understood that insert is an important part in stick-applicator assembly. It can govern the stick motion and motion transfer from the stick to the applicator. It was shown in chapter 2 that instability in the lab-scale setup can be eliminated by using top-bend

insert. Whereas, using top-bend insert in the FWTR cannot prevent instability in the lower speeds of the wheel. However, it can reduce the unstable frequency of oscillation from 847.5 Hz to 397.2 Hz under the same operational conditions. Furthermore, it can make more delay in the recurrence of the instability. As it was shown in Figure 3.3 (a), instability occurs two times within 30 seconds by using top-bend insert in the stick-applicator assembly. Whereas the recurrence of instability was more than two when the regular insert was in use (Figure 3.2 (a)).

Increasing the wheel speed causes the stable forced vibration. Harmonics of the wheel speed (600 rpm or 10 Hz) in the stick response illustrated in Figure 3.4 may have to do with the nonlinear friction force in the interface and intrinsic nonlinear behavior of the stick-applicator assembly. It is worth mentioning that instability was not observed in higher speeds but high level of forced vibration existed in the stick-applicator assembly due to motion transfer from the wheel to the stick through friction coupling.

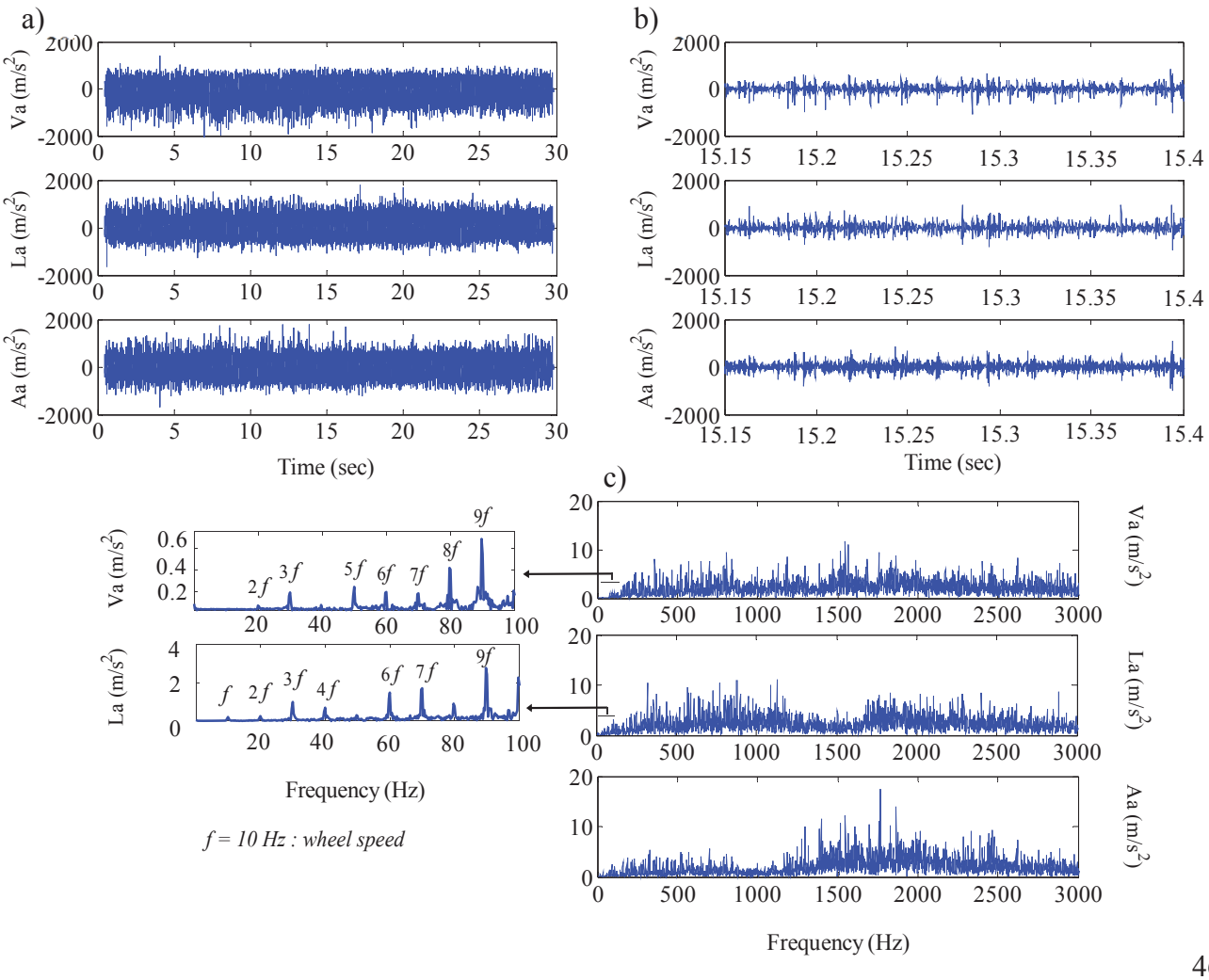

Figure 3.4 : Stick's acceleration at 600 rpm and regular insert in use; (a) total measurement, (b) detail of the signal in time domain, (c) FFT of response of b (Observation of wheel speed harmonics)

As pointed out earlier, occurrence of instability in lower speeds (less than 10 rpm) is not of great importance since the wheel rotates higher than 10 rpm most of the time and stable forced vibration is the common type of motion in the applicator- wheel assembly. Therefore, comparison between Rms values of stick-applicator assembly incorporating four different inserts at wheel speeds higher than 10 rpm may illuminate the efficacy of the insert designs in suppressing the forced vibration arising from applicator- wheel interaction. Figure 3.5 shows the variation of the Rms values of stick and the applicator at different speeds by using different inserts. Each experiment at every speed was repeated three times to make sure the trend is consistent. In the figure below, the average Rms values of accelerations are reported.

a)

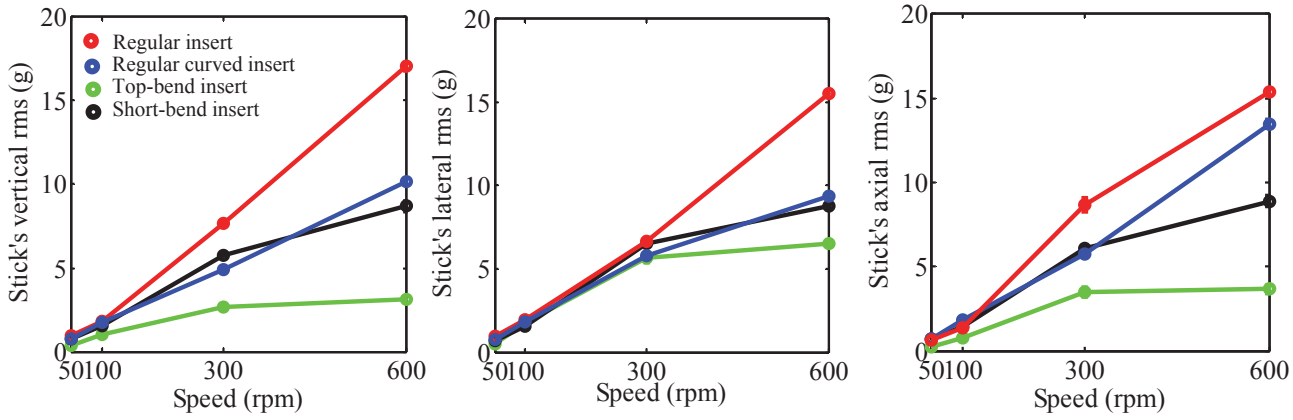

b)

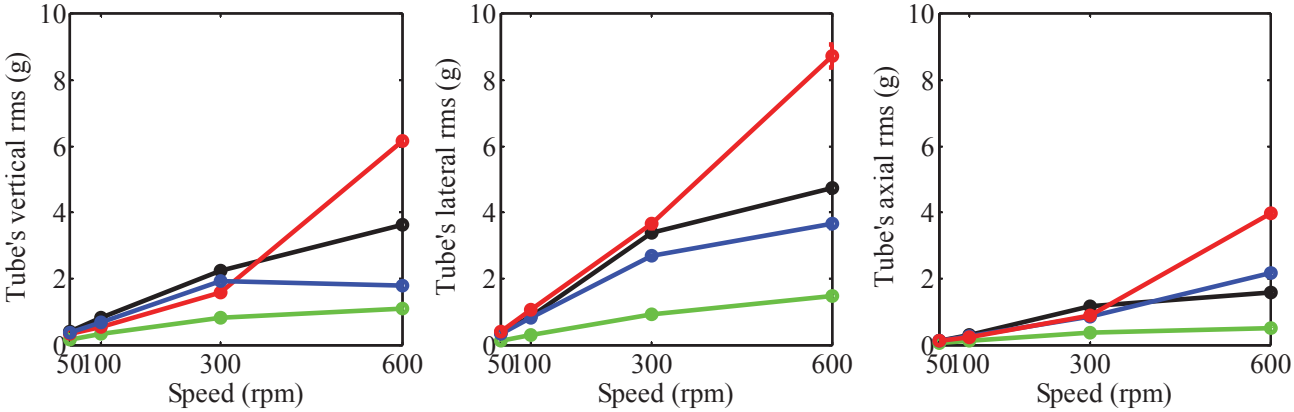

Figure 3.5 : (a) Stick's Rms (g) of different inserts at different wheel speeds; (b) tube's Rms (g) of different inserts at different wheel speeds.

3.3 Discussion

As mentioned earlier, lab-scale setup has some limitations which do not exist in the FWTR. Low-level of input energy and lack of a flange, which may act as a lateral support in the FWTR, are the main restrictions of the lab-scale setup. Therefore, evaluation of findings based on the lab-scale setup needs to be done on the FWTR.

Experiments conducted on the lab-scale setup and FWTR demonstrated that portion of the stick motion transfers to the applicator. According to the lab-scale setup, insert was shown to be an effective part in eliminating the instability and suppressing the vibration. To check the efficacy of the insert designs, FWTR was exploited. Instability occurred in the FWTR at the lower speeds. It was shown that insert modification can reduce the frequency of the unstable oscillation and make more delay in the recurrence of instability. However, insert modification could not eliminate the instability. Furthermore, it was observed that increasing the wheel speed results in the forced vibration. Therefore, fatigue-related problems due to forced vibration are the main concern in the stick-applicator assembly. In that regard, four different inserts were tested to assess their efficacy in suppressing the vibration. It can be understood from Figure 3.5 that when wheel speed is less than 600 rpm, top-bend insert is more capable of suppressing the vibration in the stick-applicator assembly and compensating itself for stick motion compared with the other insert designs. Short-bend insert seems not to be as effective as it was in the lab-scale setup in decreasing the vibration in the stick-applicator assembly. Although FWTR and lab-scale setup experiments confirm the inappropriate performance of the regular insert to lower the vibration, to understand accurately the usefulness of the insert designs, fatigue tests should be conducted and S-N diagrams are required to be found [47,48]. For instance, the tube's Rms value (g) in vertical direction at 600 rpm for regular insert, regular curved insert, top-bend insert and short –bend insert is 6.1, 1.88, 1.088 and 3.61 respectively. Fatigue tests answer how the differences between the Rms values influence on the induced stress of the tube and eventually failure of the tube. Conducting the fatigue tests and finding the S-N curves are proposed topics for future studies.

Chapter 4: Conclusions and Future works

Chatter/Squeal was recognized as an inconsistent and random phenomenon in the field experiments (i.e. when bogie, wheel and rail are in connection to each other). Experiments conducted on the full-wheel rig in Chapter 4 confirmed the claim made by Sharma [22], saying that most of the vibration in the stick-wheel interaction is forced vibration. Therefore, it is reasonable to conclude that rotational motion of the wheel, as a source of energy in stick-wheel interaction, may not be the main reason of producing instability in the field experiments. Wheel suspension motion as another source of energy in the stick-wheel interaction could be responsible of producing instability in the field experiments. In this regard, the lab scale setup, which uses mock-wheel to simulate up and down and transverse motion was designed to produce consistent instability. Lab-scale setup helps examine the behavior of the stick-applicator assembly during instability. Furthermore, understanding the ways to lower vibration in stick-applicator assembly by identifying the main contributing parts can be achieved through the lab-scale setup.
To better analyze the dynamics of the lab-scale setup:

- First, the dynamics of each subsystem used in the lab-scale setup was studied and it was shown by various experiments that both substructures are able to represent nonlinear behavior when they are subject to certain level of input force.
- Having known the characteristics of each substructure, the dynamics of the coupled system was investigated. It was found that
    - Period doubling bifurcation occurs consistently in certain ranges of excitation frequencies and above certain excitation voltages for the interlocking sticks inside the applicator.
    - Lateral stiffness could be one of the controlling design parameters of the lab-scale setup to decrease the vibration level.
    - More numbers of short interlocking sticks inside the applicator, the less the required threshold for instability is in the coupled system. Moreover, vibration reduction by using one long stick in the coupled system, experimentally proved the

necessity of thinking about new interlocking stick designs for future studies to minimize the impact of looseness between sticks on the lateral stiffness of the sticks.

- The regular insert could have been the best insert design if no gap existed in the stick-applicator assembly. Furthermore, comparison made between the vibration level of stick-applicator assembly using four different inserts revealed the significance of insert modifications in suppressing the vibration of the coupled system.

Finding a mathematical model for the lab-scale setup to substantiate the observed nonlinear behaviors needs to be done by future studies.

Low-level of input energy and lack of having a flange, which may act as a lateral support in the FWTR, are the main restrictions of the lab-scale setup. Therefore, the efficacy of the new insert designs was tested on the full wheel test rig. It was found that top-bend insert, which was requested to be designed during the present project, is more capable of suppressing the vibration in stick-applicator assembly and compensating itself for stick motion compared with the other insert designs. However, to clarify accurately the practicality of the insert designs, fatigue tests should be conducted and S-N curves are required to be found for the stick-applicator assembly with different inserts by the future studies.

Furthermore, the disparities between tube and stick acceleration levels among different insert designs need to be carefully understood by investigating the transmissibility plots in future studies.

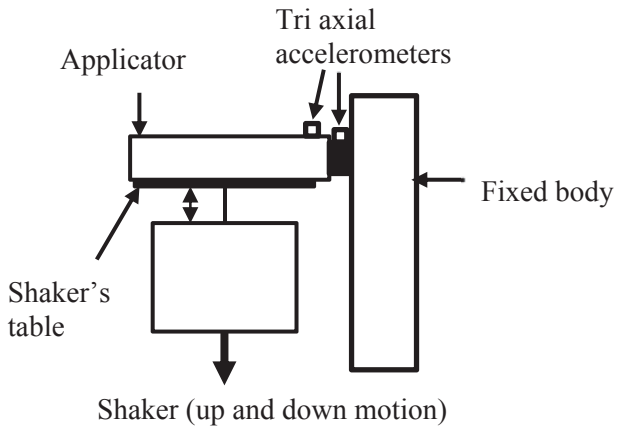

Figure 4.1 : Proposed lab-scale setup to study the effect of suspension motion of the stick-applicator assembly

As mentioned earlier, the other source of producing vibration in the stick-applicator assembly is the suspension motion of the stick-applicator assembly which was neglected during this project. The experiment depicted in Figure 4.1 can be carried out to gain more understanding of stick-applicator assembly and the significance of the suspension motion. As shown in the Figure 4.1, the stick-applicator assembly is mounted on the shaker capable of providing up and down motion and sticks are in contact with the fixed structure. Thereby, tube is prone to failure due to motion transfer of the shaker, which acts as the suspension motion, and stick-applicator interaction. Considering an appropriate suspension for the FWR experiments may also illuminate the impact of suspension motion on the instability which was observed inconsistently in the field experiments.

The long term plan for this research is to have structurally robust solid stick friction control systems by optimizing the required design changes. In that regard, the findings of this research could be used to improve the stick-applicator assembly performance in the wheel-rail industry.

Bibliography

[1] Lewis, R. and Olofsson, U. eds., 2009. *Wheel-rail interface handbook*. Elsevier.

[2] Sharma, C.P., 2011. *Friction induced vibrations in railway transportation* (MASc thesis, University of British Columbia)

[3] Stock, R., Stanlake, L., Hardwick, C., Yu, M., Eadie, D. and Lewis, R., 2016. Material concepts for top of rail friction management–Classification, characterisation and application. *Wear*, *366*, pp.225-232.

[4] Kalousek, J. and Johnson, K.L., 1992. An investigation of short pitch wheel and rail corrugations on the Vancouver mass transit system. *Proceedings of the Institution of Mechanical Engineers, Part F: Journal of Rail and Rapid Transit*, *206*(2), pp.127-135.

[5] Berger, E.J., 2002. Friction modeling for dynamic system simulation. *Applied Mechanics Reviews*, *55*(6), pp.535-577.

[6] Ibrahim, R.A., 1994. Friction-induced vibration, chatter, squeal, and chaos—part II: dynamics and modeling. *Applied Mechanics Reviews*, *47*(7), pp.227-253.

[7] Kinkaid, N.M., O'reilly, O.M. and Papadopoulos, P., 2003. Automotive disc brake squeal. *Journal of sound and vibration*, *267*(1), pp.105-166.

[8] Sheng, G., 2007. *Friction-induced vibrations and sound: principles and applications*. CRC press.

[9] Oberst, S. and Lai, J.C.S., 2011. Chaos in brake squeal noise. *Journal of Sound and Vibration*, *330*(5), pp.955-975.

[10] Jarvis, R.P. and Mills, B., 1963. Vibrations induced by dry friction. *Proceedings of the Institution of mechanical Engineers*, *178*(1), pp.847-857.

[11] Chen, G.X., Zhou, Z.R., Kapsa, P. and Vincent, L., 2003. Experimental investigation into squeal under reciprocating sliding. *Tribology International*, *36*(12), pp.961-971.

[12] Lin, Y.Q. and Wang, Y.H., 1991. Stick-slip vibration of drill strings. *Journal of Engineering for Industry*, *113*(1), pp.38-43.

[13] Zhu, Xiaohua, Liping Tang, and Qiming Yang, "A literature review of approaches for stick-slip vibration suppression in oilwell drillstring," *Advances in Mechanical Engineering,* pp. 952-967

[14] Murakami, Hideto, Naomasa Tsunada, and Terukiyo Kitamura., "A study concerned with a mechanism of disc-brake squeal.," *SAE Technical Paper,,* 1984

[15] Akay, A., Giannini, O., Massi, F. and Sestieri, A., 2009. Disc brake squeal characterization through simplified test rigs. *Mechanical systems and signal processing*, *23*(8), pp.2590-2607.

[16] Chen, F., Chern, J. and Swayze, J., 2002. *Modal coupling and its effect on brake squeal* (No. 2002-01-0922). SAE Technical Paper.

[17] Hoffmann, N. and Gaul, L., 2003. Effects of damping on mode-coupling instability in friction induced oscillations. *ZAMM-Journal of Applied Mathematics and Mechanics/Zeitschrift für Angewandte Mathematik und Mechanik: Applied Mathematics and Mechanics*, *83*(8), pp.524-534.

[18] Bigoni, D. and Noselli, G., 2011. Experimental evidence of flutter and divergence instabilities induced by dry friction. *Journal of the Mechanics and Physics of Solids*, *59*(10), pp.2208-2226

[19] Ziegler, H., 1953. Linear elastic stability. *Zeitschrift für angewandte Mathematik und Physik ZAMP*, *4*(2), pp.89-121.

[20] Duffour, P. and Woodhouse, J., 2004. Instability of systems with a frictional point contact. Part 1: basic modelling. *Journal of Sound and Vibration*, *271*(1-2), pp.365-390.

[21] Altintaş, Y. and Budak, E., 1995. Analytical prediction of stability lobes in milling. *CIRP Annals-Manufacturing Technology*, *44*(1), pp.357-362.

[22] Sharma, C.P. and Phani, A.S., 2015. Stability analysis of on-board friction modifier systems at the wheel–rail interface. *Journal of Vibration and Acoustics*, *137*(5), p.051007.

[23] Leine, R.I., Glocker, C. and Van Campen, D.H., 2001, September. Nonlinear dynamics of the woodpecker toy. In *Proceedings of DETC 2001 ASME Symposium on Nonlinear Dynamics and Control In Engineering Systems* (pp. CDROM-9).

[24] Pavlovskaia, E., Wiercigroch, M., Woo, K.C. and Rodger, A.A., 2003. Modelling of ground moling dynamics by an impact oscillator with a frictional slider. *Meccanica*, *38*(1), pp.85-97.

[25] Ibrahim, R.A., 2009. *Vibro-impact dynamics: modeling, mapping and applications* (Vol. 43). Springer Science & Business Media.

[26] Ema, S. and Marui, E., 2000. Suppression of chatter vibration of boring tools using impact dampers. *International Journal of Machine Tools and Manufacture*, *40*(8), pp.1141-1156.

[27] Ema, S. and Marui, E., 1998. Suppression of chatter vibration in drilling. *Journal of manufacturing science and engineering*, *120*(1), pp.200-202.

[28] Shaw, S.W., 1985. Forced vibrations of a beam with one-sided amplitude constraint: theory and experiment. *Journal of Sound and Vibration*, *99*(2), pp.199-212.

[29] Moon, F.C. and Shaw, S.W., 1983. Chaotic vibrations of a beam with non-linear boundary conditions. *International Journal of non-linear Mechanics*, *18*(6), pp.465-477.

[30] Nayfeh, A.H. and Mook, D.T., 2008. *Nonlinear oscillations*. John Wiley & Sons.

[31] Cartmell, M., 1990. *Introduction to linear, parametric, and nonlinear vibrations*. Chapman and Hall

[32] Jia, Y. and Seshia, A.A., 2014. An auto-parametrically excited vibration energy harvester. *Sensors and Actuators A: Physical*, *220*, pp.69-75

[33] Daqaq, M.F., Masana, R., Erturk, A. and Quinn, D.D., 2014. On the role of nonlinearities in vibratory energy harvesting: a critical review and discussion. *Applied Mechanics Reviews*, *66*(4), p.040801.

[34] Haddow, A.G., Barr, A.D.S. and Mook, D.T., 1984. Theoretical and experimental study of modal interaction in a two-degree-of-freedom structure. *Journal of Sound and Vibration*, *97*(3), pp.451-473

[35] Balachandran, B. and Nayfeh, A.H., 1991. Observations of modal interactions in resonantly forced beam-mass structures. *Nonlinear Dynamics*, *2*(2), pp.77-117.

[36] Nayfeh, A.H. and Balachandran, B., 2008. *Applied nonlinear dynamics: analytical, computational, and experimental methods*. John Wiley & Sons.

[37] Virgin, L.N., 2000. *Introduction to experimental nonlinear dynamics: a case study in mechanical vibration*. Cambridge University Press.

[38] Ewins, D.J., 1984. *Modal testing: theory and practice* (Vol. 15). Letchworth: Research studies press.

[39] Kerschen, G., Worden, K., Vakakis, A.F. and Golinval, J.C., 2006. Past, present and future of nonlinear system identification in structural dynamics. *Mechanical systems and signal processing*, *20*(3), pp.505-592.

[40] Londoño, J.M., Neild, S.A. and Cooper, J.E., 2015. Identification of backbone curves of nonlinear systems from resonance decay responses. *Journal of Sound and Vibration*, *348*, pp.224-238.

[41] Feldman, M., 1994. Non-linear system vibration analysis using Hilbert transform--I. Free vibration analysis method'Freevib'. *Mechanical systems and signal processing*, *8*(2), pp.119-127.

[42] Noël, J.P., Renson, L. and Kerschen, G., 2014. Complex dynamics of a nonlinear aerospace structure: experimental identification and modal interactions. *Journal of Sound and Vibration*, *333*(12), pp.2588-2607.

[43] Zavodney, L.D., 1991. Identification of nonlinearity in structural systems: Theory, simulation, and experiment. *Applied Mechanics Reviews*, *44*(11S), pp.S295-S303.

[44] Shaw, S.W. and Holmes, P.J., 1992. A periodically forced piecewise linear oscillatort. *Chaotic Oscillators: Theory and Applications*, *90*(1), p.304.

[45] Sarkar, S., Venkatraman, K. and Dattaguru, B., 2004. Dynamics of flexible structures with nonlinear joints. *Journal of vibration and acoustics*, *126*(1), pp.92-100.

[46] Chen, G.X. and Zhou, Z.R., 2005. Experimental observation of the initiation process of friction-induced vibration under reciprocating sliding conditions. *Wear*, *259*(1-6), pp.277-281.

[47] Lee, Y.L., Pan, J., Hathaway, R. and Barkey, M., 2005. *Fatigue testing and analysis: theory and practice* (Vol. 13). Butterworth-Heinemann.

[48] Weibull, W., 2013. *Fatigue testing and analysis of results*. Elsevier.

Appendices

Appendix I

Coherence function in frequency domain is defined as

$$\gamma(\omega)^2 = \frac{|S_{xy}(\omega)|^2}{S_{xx}(\omega)S_{yy}(\omega)}$$

$S_{xx}(\omega)$: autocorrelation of the input, $S_{yy}(\omega)$: autocorrelation of the output, $S_{yy}(\omega)$: cross correlation of the input and the output .

The coherence magnitude at each frequency is between 0 and 1. A coherence of 1.0 indicates that the output is purely and linearly explained by the input. Deviation from unity may be the indication of noise in input or output, a non-linear behavior and/or any combination of them. Figure below shows the lateral accelerance of the mock-wheel due to lateral impulse on the tip mass. Good coherence exists at the resonance peak around 12.5 Hz.

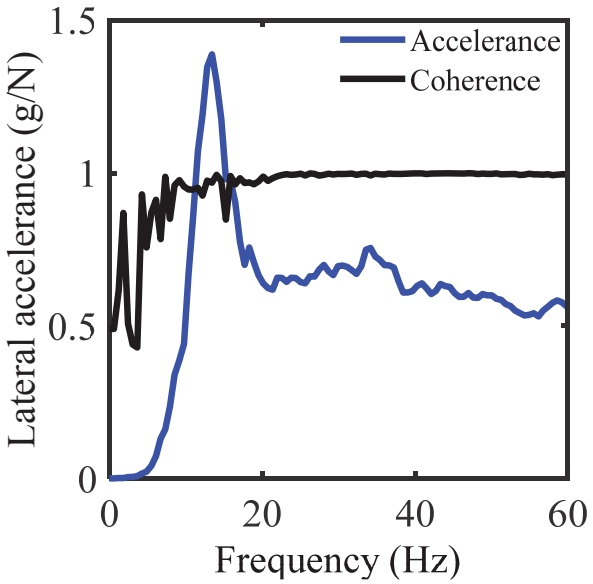

Figure 1 : Impact hammer test with coherence

Appendix II

Stiffness of the shaker can be found based on the experiment depicted below.

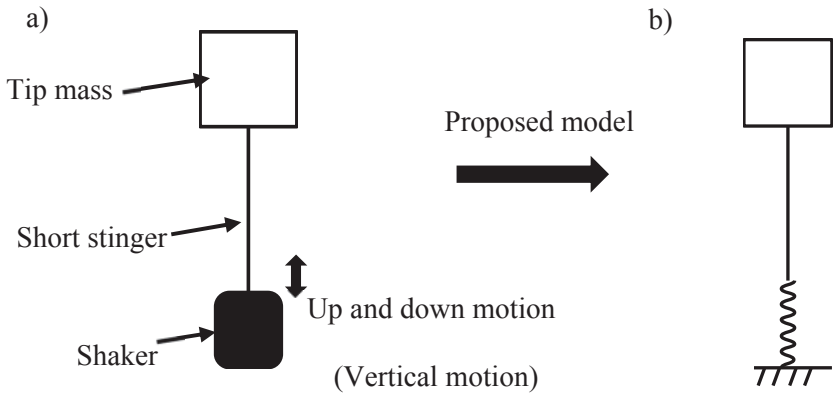

Figure 2 : (a) Schematic of experimental setup to measure the stiffness of the shaker, (b) proposed model

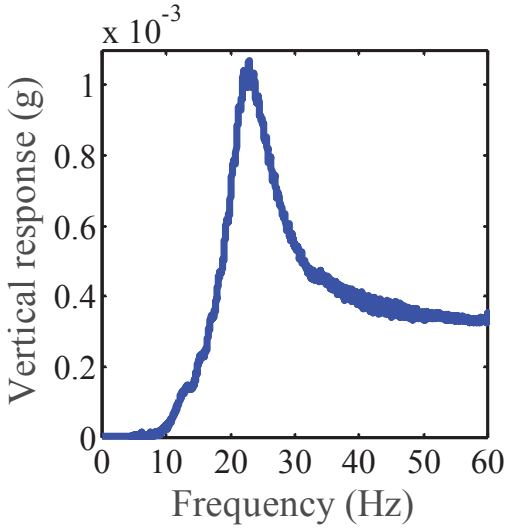

Figure 3: Frequency spectrum of the tip mass in vertical direction

The vertical response of the tip mass was measured and it is illustrated in Figure 3. A vertical mode exists at 22.04 Hz. Short stinger connected to the tip mass has flexible modes well above 100 Hz. Therefore, the mode at 22.04 is a rigid body mode in the system. The mass of the moving element in the shaker is negligible compared with the total mass of tip mass and stinger which is 165 grams. Therefore, stiffness of the shaker can be calculated as follows.

$$\omega^2 = \frac{k_{shaker}}{m_{total}} \rightarrow k = 0.165 \times (22.04 * 2 * 3.14)^2 = 3161\ N/m$$

3161 N/m is very close to a number announced by shaker's manual as suspension axial stiffness for the shaker which is 3150 N/m. Therefore, 3150 was used in FEM of the mock-wheel. It is worth mentioning that no significant change in the linear modes of the mock-wheel modelled in ABAQUS occurs by changing 3150 to 3160 as shaker's stiffness.